water

MDPI

Article

Development of Pleistocene Fluvial Terraces on the Eastern Frontal Sector of the Southern Apennines Chain, Italy

Paolo Giannandrea [1], Salvatore Ivo Giano [1,*] and Roberto Sulpizio [2]

[1] Dipartimento di Scienze, Università degli Studi della Basilicata, Viale dell'Ateneo Lucano 10, I–85100 Potenza, Italy
[2] Dipartimento di Scienze della Terra e Geoambientali, Università degli Studi di Bari "Aldo Moro", via Orabona 4, 70125 Bari, Italy
* Correspondence: ivo.giano@unibas.it; Tel.: +39-0971-798542

Received: 13 May 2019; Accepted: 27 June 2019; Published: 28 June 2019

Abstract: The investigation of Pleistocene fluvial terraces in the small river valley of the Pescogrosso Stream and surrounding areas has shown a complex and positive location for the study of a fluvial catchment development. The Pescogrosso Stream is a left tributary of the Sinni River and is placed on the eastern front of the fold-and-thrust belt of the southern Apennine chain of Italy. Sedimentological and geomorphological analyses of eight fluvial terraced units revealed that their formation and evolution were strictly controlled by regional tectonic uplift of the Ionian arc, by climatic changes, and by sea-level variations. In particular, the Ionian sea-level oscillations, as a factor in controlling the short-term fluvial terrace development, was the main factor responsible for the three older terraces' evolutions. Conversely, the evolution of the five younger terraces seems to have been controlled by the base-level variations of the Sinni River. Finally, the matching of much information derived from regional and local tectonics, the plot of longitudinal terrace profiles, and the application of a sequence-stratigraphic approach to fluvial depositional sequences allowed the recognition of three evolutionary stages of development in the Pescogrosso fluvial incised-valley system during Pleistocene times.

Keywords: fluvial terraces; sedimentology; geomorphology; Pleistocene; southern Apennines

1. Introduction

River terraces are globally distributed landforms, which localize along river valley sides and form in a variety of climatic and tectonic settings [1–15]. Flat surfaces of fluvial terraces are bounded by sloping surfaces, and their formation requires first the aggradation of both channel and floodplain sediments, and then the vertical incision of either the valley infill or the bedrock [1]. Ongoing efforts have been made to assess the relative role played by climate, sea-level changes, and tectonics on river terrace formation [1–13]. The long-term fluvial evolution (ca. 10^6 My) is strongly regulated by the lowering of both regional and local base levels, which both depend upon tectonic uplift rates. By contrast, the short-term evolution (ca. 10^4 My) is controlled by both climate and sea-level changes. In the upstream portion of the fluvial catchments, far from sea level, cold periods are characterized by both intense aggradation and incision due to the intense landscape fluvial dynamics. By contrast, during moist and stable interglacial periods, rivers tend to incise into cohesive floodplain deposits. In particular, the vertical incision of rivers seems to have mainly happened in transition times from cold to warm conditions [3,13]. Focusing on the Mediterranean fluvial catchments, multiple aggradation episodes took place during interglacial periods such as those occurring at OIS5 [9]. These episodes

were related to two main factors—the closeness of the forest ecotone to the littoral catchments, and the slight climatic changes that favored slope vegetation, hence slope stability. High relief of the upstream catchments furnished a ready supply of coarse bed deposits [9]. In the downstream fluvial valleys, floodplain aggradation and/or incision were controlled by marine base-level variations, which in turn were driven by glacioeustastic sea-level fluctuations [3,13]. In the coastal-fluvial plain areas, rivers might have formed incised-valley systems, individually comprised of an incised valley and its depositional infill, which were influenced by transgressive/regressive sea-level variations [14–17]. In active tectonic settings in which sea-level oscillation, climate change, and tectonic uplift interact one another, the fluvial system [2] can carve strath terraces in bedrock channels and fill terraces in valley floors [7,11,12].

Considering the Apennines fold-and-thrust belt of Italy, the role played by tectonics, climate, and sea-level changes in the formation of fluvial terraces during Pleistocene times is still debated [18–24]. A Quaternary uplift of about 0.3–1.0 mm/year was computed for both northern and central Apennines by using different approaches and tools [18,22–25]. Taking fluvial terraces into account, several authors documented how both tectonic uplift and climate variations triggered headward erosion and stream piracy [19,21]. Accordingly, they both contributed to relief production, suggesting a near-attainment of dynamic equilibrium between tectonic uplifts and erosional processes [19]. A quite similar uplift rate of 0.5–0.6 mm/year was computed for the last 700 ky [26,27] in the southern Apennines by considering the faults displacing different landforms and hence active within the aforementioned time span [28]. Consequently, it is inferred that the southern Apennines do not exhibit a steady-state condition [27]. Focusing on the differential uplift of the eastern portion of southern Apennines belt visible at the Tolve village and Valsinni Ridge area, it was investigated by using fluvial terrace arrangements as passive markers of tectonic deformation [20], and by computing morphometric parameters [29]. Indeed, the uplift stages estimated for the Valsinni Ridge are consistent with a bedrock incision rate varying from 1.2 mm/year (ca. 400 ky) to 0.6–1.0 mm/year (ca. 240 ky) [20]. In this work, we investigate the contribution provided by climate, tectonics, and sea-level oscillations in the formation and development of Pleistocene fluvial terraces, which are in the easternmost thrust front of the southern Apennines. For this purpose, we match geomorphological and stratigraphic data pertaining to the Pescogrosso Stream valley and surrounding areas of the Basilicata Region of Italy. We use information extracted from the depositional architecture and sedimentological features of fluvial deposits cropping out in the study area. Data are merged with those obtained after geomorphological analysis of the terrace profiles. Then, a comparison of the results with those of the Ionian marine terraces permits a computation of the absolute age of fluvial terraces from the Marine Isotope Stage (MIS) curve. Furthermore, a better constraint for the absolute dating of the fluvial deposits is provided by the tephra horizon documented for the first time in the study area. Results presented in this work hence shed new light into the role played by climate and sea-level variations in the fluvial terraces evolution in the eastern portion of the southern Apennines.

2. Outlines of the Study Area

2.1. Regional Geology and Geomorphology

The southern Apennines chain (Figure 1a) represents an Adriatic-verging fold-and-thrust belt derived from the deformation of Mesozoic–Cenozoic circum-Tethyan domains and associated Neogene–Pleistocene foredeep and satellite-basin deposits ([30] and references therein). The most recent shortening occurred on the front range of the chain deforming the Pleistocene sediments and volcanics [29,31,32]. Moreover, extensional tectonics displacing the orogeny is still active along the axis of the Apennines chain [26–39]. The average direction of the chain axis is approximately N150°, which corresponds to the strike of both the main thrusts and the coaxial normal faults. Such a complex structural setting produced a mountain chain over 2000 m high and a watershed NW-SE-oriented that separates the drainage network toward the Tyrrhenian Sea (south-west), Adriatic Sea (north-east), and

the Ionian Sea (east). The chain can be roughly divided into three zones—the inner, the axial, and the outer belts (a, b, and c respectively in Figure 1) parallel to its NW-SE elongation axis. The inner belt (a in Figure 1b) corresponds to the Tyrrhenian side of the Apennines and is composed of Cretaceous to Oligocene deep-sea pelagic successions (Liguride and Sicilide units, [40]) overthrusted on Mesozoic shallow-water carbonate units forming the Cilento Promontory with a maximum elevation at Cervati Mt. (1900 m a.s.l.). The axial belt (b in Figure 1b) is formed of Mesozoic to Cenozoic platform carbonate units overthrusted on the coeval deep-sea water pelagic units [30,41]. Miocene flysch and clastic deposits of Pliocene thrust-top basins, both involved in compressive deformation, lie unconformably on these tectonic units. Quaternary tectonics is still active along the axial zone of the chain and generated tectonically induced intermontane basins [26,33,39,42,43]. Many mountain tops of the axial belt correspond to the remnants of Pliocene–Pleistocene erosional land surfaces uplifted and dismembered by Quaternary faults [28]. The landscape of the axial zone includes block-faulted ridges and massifs, bounded by high-angle fault scarps retreated by slope-replacement processes [44] and displaced by active faults [38]. The intermontane basins filled with Pliocene–Quaternary fluvial and lacustrine deposits [36,45] are also present. The fluvial network following the strike of geological structures transversally cuts the bedrock and flows into the Tyrrhenian, Adriatic, or Ionian seas. The outer belt of the chain (c in Figure 1b) is made of Cenozoic sandstones, marls, and clays forming the eastern imbricate fan of the orogenic wedge. Its frontal zone tectonically overlaps the Pliocene–Pleistocene clastic deposits of the Bradano Foredeep and is locally buried by such sediments. The outer belt is characterized by a lack of extensional block faulting and shows a general passive northeastward tilting, because of the uplift of the chain. This is also supported by the main rivers that flow perpendicularly or obliquely to the strike direction of the main tectonic structures and following the regional slope of the belt eastward [29,46]. The hilly landscape of the outer belt does not exceed 1100 m of elevation a.s.l. and fluvial valleys are oriented from NE–SW, in the northern sector, to E–W, in the southern sector, transversally cutting the chain. Eastward, the outer belt is bounded by the marine to fluvial plain of the Bradano Foredeep.

Pliocene–Pleistocene sedimentary infill of the Bradano Foredeep is constituted by a transgressive–regressive clastic sequence of conglomerate, sand, and clay several thousand meters thick [47–50]. The sinking of the area occurred during Early Pleistocene, and was responsible for the deposition of marine clays, unconformably overlaid by Middle to Upper Pleistocene; coarsening upward deposits constituted of marine to continental silt, sand, and conglomerate. The Bradano Foredeep is characterized by a medium- to low-relief landscape, featured by gently dipping surfaces, less than 3–5° of slope angle, separated by high-angle scarps, representing relics of Middle Pleistocene to Holocene staircase marine terraces (Figure 2a) [27,46–56]. Many authors have debated the number and age of the Ionian marine terraces, and there is no general agreement, mainly because of the bad condition of outcrops. The number of terraces varies from one single terrace, faulted and displaced in several surfaces by tectonic activity [57], to five/seven [27,53–56] and ten/eleven [51,52]. Moreover, many dating methods on terraced marine deposits have been carried out, and different chronological correlations to MIS stages have been proposed in the literature [51–58]. According to Westaway et al. (2007) [27], the marine terrace formation was related to climatic inputs based on Milankovitch forcing, in association with regional uplift. The authors suggested that uplift and dissection of the study area might be attributed to isostatic consequences of Middle–Late Pleistocene erosion, and not to a crustal deformation. Recently, integrated analysis of the drainage network, statistical properties of the landscape, morphostructural analysis, and evaluation of geomorphic indices in the whole Bradano Foredeep area have provided new constraints on the late Quaternary evolution of the area [46]. The development of Ionian hydrographic network is due to a propagation toward east-northeast and southeast, respectively, of the blind-thrusts affecting the eastern segment of southern Apennines chain. The trellis-type fluvial network of the Bradano, Basento, Agri, and Sinni drainage basins cuts the marine terraces. The regional and local uplifts of the chain produced base-level lowering that triggered the formation of the fluvial network pattern, thus producing the progressive entrenchment of rivers in the Bradano Foredeep deposits.

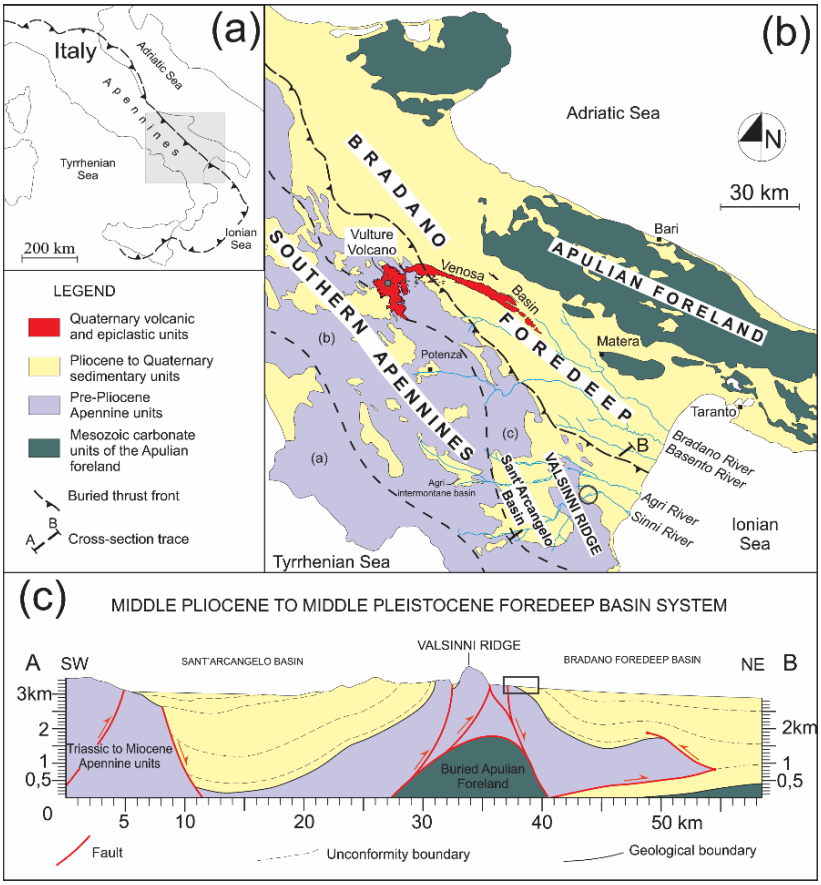

Figure 1. Location of the study area (**a**); geological sketch map of southern Italy (**b**) and geological cross-section (**c**) of the eastern front of southern Apennine chain (modified after [20,30]). Circle in (**a**) and rectangle in (**b**) indicate the investigated area. Please note that the vertical scale in (**c**) does not refer to the elevation a.s.l.

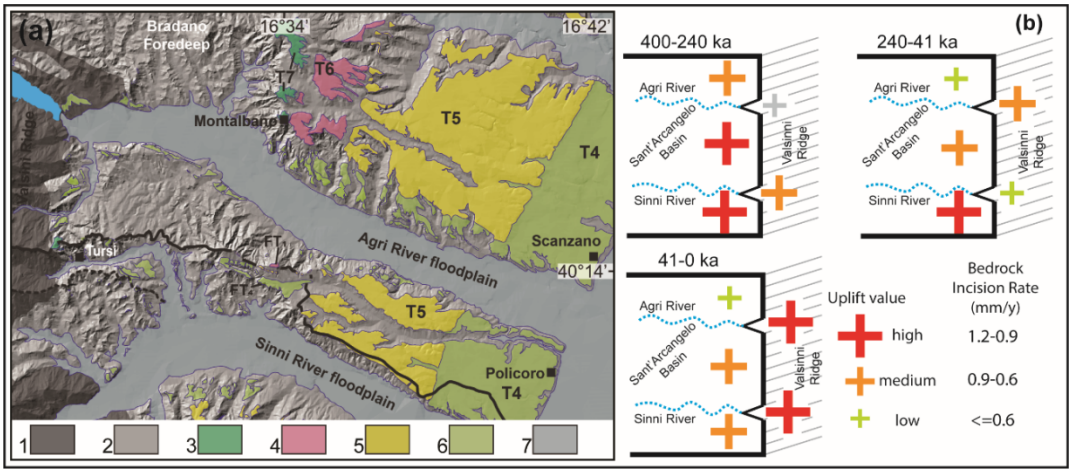

Figure 2. (**a**) Sketch map of marine terraces between Montalbano and Policoro villages (modified after [49]). Legend: 1. bedrock of the south Apennines chain; 2. Bradano Foredeep area; 3, 4, 5, 6. T7 to T4 orders of marine terraces, respectively; 7. Agri and Sinni rivers floodplains. (**b**) Differential tectonic uplift in the eastern sector of Sant'Arcangelo Basin and in the Valsinni Ridge during the last 400 ka (modified after [20]).

2.2. The Pescogrosso Catchment and Surrounding Areas

The Pescogrosso Stream is a left tributary of the Sinni River and cuts, from west to east, the eastern slope of the Valsinni Ridge. This latter Ridge is a NW-trending anticline forming a morphological threshold of two distinct sedimentary domains: the Sant'Arcangelo Basin toward west, and the Bradano Foredeep toward east (Figure 1b,c). The Pescogrosso Stream, in the upstream reach, flows east, whereas at Ponte Masone in the downstream reach it changes the course by about 90° toward south (Figure 3). The drainage basin of Pescogrosso Stream shows about 700 m of relief, suggesting high potential energy and its slope is distributed on average values mainly ranging from 1° to 20°. The fluvial pattern is trellis-type and shows small tributaries mainly running on the left-side valley, because of its regular and higher slope than the right-side one. The Pescogrosso Stream valley, in the lowermost reach and below the fluvial elbow, shows a floodplain that varies from 500 to 1000 m in width and forms a poorly incised alluvial fan at the mouth. The upstream valley was carved on clays with interbedded calcarenites and marly carbonate of the Sicilide Unit [40] representing the sedimentary core of the Valsinni Ridge anticline, and on marls, arenite, and sandy-clay clastic deposits forming the Miocene and Pliocene sedimentary covers of the Valsinni Ridge (Figure 3). In the middle and low catchments, the Pescogrosso Stream flows on Quaternary clayey-sandy deposits of the Bradano Foredeep, composed of marine sands with interbedded conglomerate lenses dipping from 30° to 5° or also 0° toward north-eastern. A well-developed N-S-striking high-angle fault cuts these two groups of sedimentary units. The Valsinni Ridge anticline was grown on the Apulian Platform from Late Pliocene to Middle Pleistocene [59] and, presently, is transversally incised by the Agri and Sinni rivers. In the study area, the S. Arcangelo and Coppolo Mts. are the main mountain peaks of the ridge, reaching approximately 858 and 890 m of altitude a.s.l., respectively.

The tectonically induced differential uplift affecting the Valsinni Ridge was investigated using fluvial terraces displacement by Giano et al. (2014) [20]. The authors recognized three different Late Pleistocene uplift stages and rates in the ridge thus furnishing the spatial and temporal geomorphological evolution of both the eastern side of Sant'Arcangelo Basin and the Valsinni Ridge (Figure 2b). The uplift stages affecting the Valsinni Ridge (Figure 2b) during Late Pleistocene times have shown different bedrock incision rates varying from 1.2 mm year^{-1} at about 400 ka to 0.6–1.0 mm year^{-1} at about 240 ka [20]. The Sant'Arcangelo Basin "*Auctt*." (Figure 1b,c) is a Pliocene to Pleistocene sedimentary basin filled by marine to continental deposits up to 2500 m thick, and presents an almost rectangular shape and long-sides facing northward in plain view (Figure 1b). The basin infill is formed of conglomerate, sand, and marly clay deposits of Late Pliocene, of shelf- to open-shelf mudstone and shallow-marine sandstone deposits of Late Pliocene to Early Pleistocene, and of fluvial to lacustrine deposits of Early to Middle Pleistocene. The tectono-sedimentary evolution of Sant'Arcangelo Basin has been differently interpreted as follows: (*i*) a pull-apart basin generated by a NW-SE left-transcurrent shear zone [60], (*ii*) a piggy-back, or (*iii*) a thrust-top basin resulting from the growth of the Tursi-Rotondella anticline ridge [30,59–64]. Based on the Early Pleistocene counterclockwise vertical-axis rotations (20° in <0.5 My) [64] suggest that a left-lateral deformation was particularly effective in the Sant'Arcangelo Basin, because of the lateral break-off of the African–Ionian–Adriatic lithosphere and the rapid south-eastward slab retreat. The differential uplift of the Sant'Arcangelo Basin and Valsinni Ridge suggested by the tilting of the Agri and Sinni fluvial terraces would appears to indicate that such slab retreat processes might have persisted in the Ionian area also during Late Pleistocene [20] and could be responsible for rising of the marine terraces.

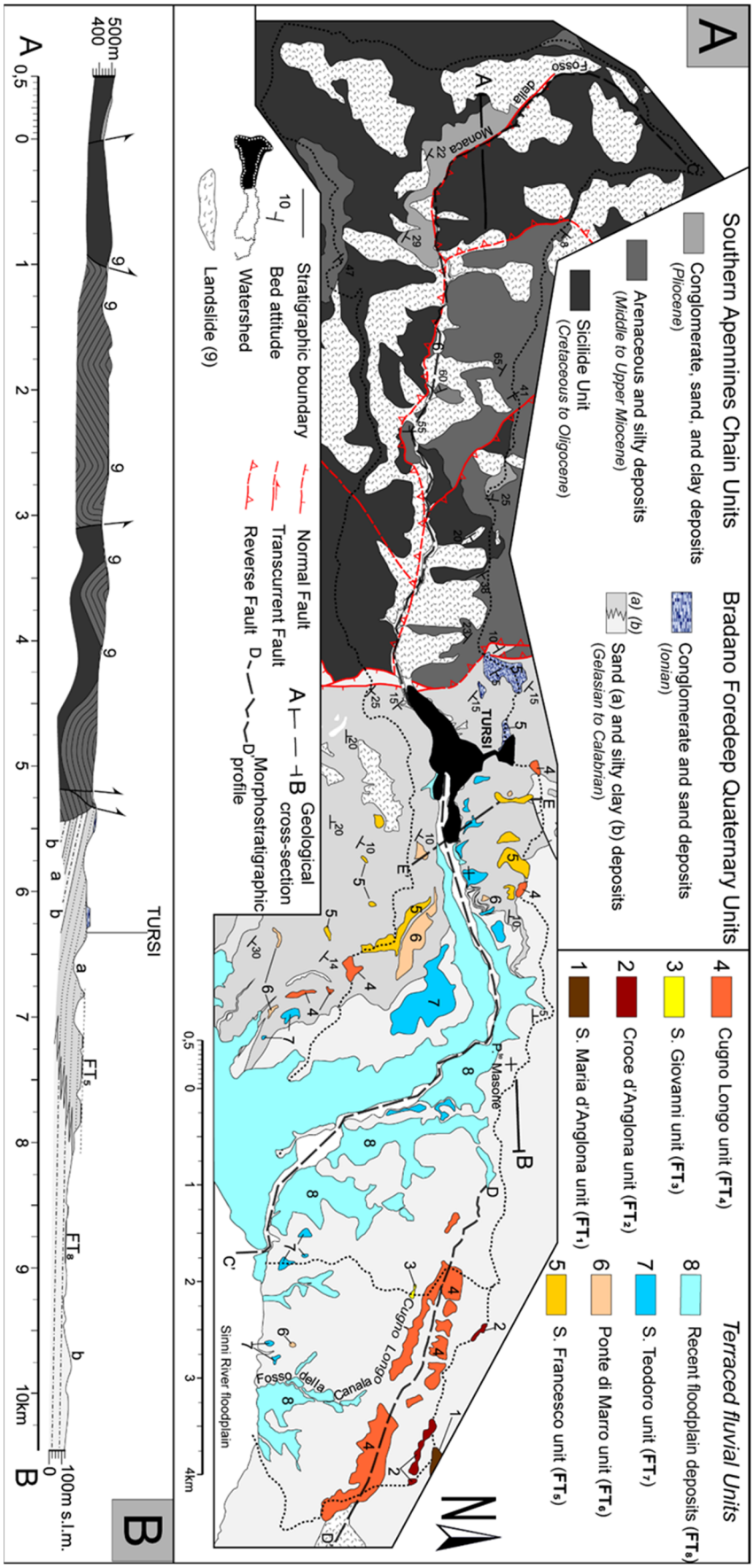

Figure 3. Geological map of the fluvial terraces outcropping in the Pescogrosso catchment and surrounding areas (**A**). Geological cross-section trough the studied area (**B**). See Figure 1 for location.

In the study area, the Bradano Foredeep landscape is featured by gently dipping surfaces (slope angles of 3–5° toward the sea) of staircase marine terraces interrupted by morphological scarps. Such marine terraces, ranging in elevation from about 400 m a.s.l. to 10–15 m a.s.l., are the sedimentary tops of uplifted coastal wedges with an internal complex stratigraphy [54]. The sedimentary top surface is deeply cutting by a minor drainage network, mainly developed according to a trellis pattern. The roughly rectangular arrangement of the drainage network is a prominent morphotectonic feature of the study area, since it appears to be related to a structural control by recent brittle tectonics [49]. According to Cilumbriello et al. (2008) [54], the tectonic behavior of the Ionian coastal area during Middle–Late Pleistocene was characterized by the interplay between three major tectonic structures, operating at different scales and different rates thus affecting different areas, which can be summarized as follows: (*i*) fold-related processes, (*ii*) wedge-rotation processes, and (*iii*) lithospheric duplexing processes.

3. Materials and Methods

Recognition and mapping of fluvial terraces were performed by the analysis of topographic maps at 1:2000 and 1:10,000 scales, by the interpretation of 1:33,000 aerial photos related to the years 1987–1990, and by detailed field surveys with a GPS instrument (Garmin GPS map 62stc). For each single terrace, both the mapping and surveying in the field allowed us to determine the deposit thickness, the basal erosion surface and the minor internal discontinuities in the fluvial unit, the plan view extension, the internal and external edges of the terraced surface, the longitudinal and transversal length of the terrace, and the sedimentary facies of the terraced deposits. It follows that if fluvial terraces are constituted of both sediment and landforms then their distinction is needed. The sedimentary sequences produced by fluvial aggradation are referred to as terrace deposits, whereas the landforms influenced by fluvial action are referred to as terrace surfaces, which includes both the strath and fill surfaces. Therefore, in a single fluvial terrace, three elements have been discriminated: (a) terrace deposit, (b) strath terrace, and (c) fill terrace. The field mapping of fluvial terraces has been led by lithostratigraphic (terrace deposit) and/or morphological (terrace surface) approaches, whereas in recent years, the use of the allostratigraphy [65] has allowed a more detailed definition of discontinuities related to terrace deposits.

Within each terraced deposit, we discriminated: (i) the basal erosion surface representing the bottom of the fluvial channel which immediately resting on the bedrock, (ii) the minor internal discontinuities that separate the different aggradational episodes in the fluvial sequence, and (iii) the sedimentary top of the terrace that corresponds to its tread. The fluvial sequences have been interpreted following the fluvial depositional facies association scheme proposed by Miall (1996) [66]. They are shown in Table 1 which contains the main lithofacies assemblage of study area and the interpretation of facies associations. Furthermore, some fluvial depositional sequences and their minor internal discontinuities have been discussed in the frame of an incised-valley system confined by a low-gradient coastal plain (*sensu* [15]). This latter is based on the assumption that rivers adjust their longitudinal profiles as response to sea-level oscillations. The use of sequence-stratigraphic concepts following the approach of [2,14–17] permitted the correlation of the fluvial base-level variations and the local high-frequency eustatic cycles of the Ionian sea level. Furthermore, a tephra layer interbedded within the fluvial terrace deposit has been sampled and chemical analysis by means of an electronic microscope was realized at the University of Pisa.

To better clarify the fluvial terraces distribution in the Pescogrosso Stream valley, some morphostratigrapic and topographic slope profiles have been carried out, running the fluvial valley longitudinally and transversally. The choice to realize topographic profiles was due to the necessity of a better correlation of the well-exposed fluvial terrace deposits, located out of the Pescogrosso drainage basin, and some marine terraces of the Ionian area. As a result, the hierarchical organization of terraces (Figure 3) and their distribution, regarding the marine terraces, has been carried out. In particular, the plot of the fluvial terrace profiles against the T6 and T5 Ionian marine terraces of

Brückner et al. (1982) [52], placed between Montalbano and Policoro villages, allowed us to realize a good geomorphological correlation.

Table 1. Facies code, lithofacies, and relative interpretation of the fluvial terraced deposits.

Facies Code	Lithofacies	Interpretation
Gcm	Massive clast-supported gravel and/or imbrication of clasts	Pseudoplastic debris flow, inertial flows and turbulent flows [59], hyperconcentrated flows [61,62]
Gmm	Massive, matrix-supported gravel	Pseudoplastic debris flow, low energy viscous flows [59]
Gcp	Clast-supported gravel with low planar crossbedding	Lateral growth of gravelly bars [59]
Gch	Clast-supported gravel with planar lamination, and/or imbrication of clasts	Gravel flows in supercritical regime; lag deposits, longitudinal bars, sieve deposits [59]
Gct	Clast-supported gravel with concave crossbedding	Channelized gravel flows [59]
Sp	Fine to coarse sand with planar stratification	Sand in sub-critical flow regime; linguoid and transverse bars, ripple marks [59]
Am	massive fine ash containing small clasts	Ash/sand flows with hyperconcentrated turbulent flow and fast sediment fall [62] during low energy stage [65]
Sh	Very fine to coarse sand with planar lamination and small isolated and/or aligned clasts	planar bed with sheet flood regime [59]
Ar	Fine gray ash with crossbedding and ripple marks	Ripples migration in sub-critical flow regime [59]
Fsl	Sand, silt, and mud with thin lamination and small ripple marks	Overbank flows [59,63,64] and/or waning flows
mA	Massive fine ash	Primary ash fall product
P	Brown silty sand containing isolated clasts and root fragments	Low-maturity palaeosoil [67]

4. Results and Interpretations

Geological field survey in the Pescogrosso drainage basin allowed us to recognize eight fluvial terrace deposits numbered from the older to the younger as FT_1 to FT_8, distributed from the divide to the mouth located in the Sinni River (Figure 3). The recognition and classification of fluvial terraces has also been done in the nearest of the Pescogrosso catchment thus to obtain a better understanding of their arrangement. In the studied area, six boulders facies, five sandy facies (Figure 4), and three pyroclastic facies following the approach of Miall (1996) [66] (Table 1) have been discriminated. Stratigraphic analyses and sedimentology have not been performed on the FT_3, FT_6, and FT_8 terraces because of their bad outcrops. In any case, some stratigraphic information is coming from these terraces. The FT_3 basal erosion surface is found at 225–230 m of elevation a.s.l., and the FT_3 deposit is composed of clast-supported gravel with red sandy matrix and about 15 m thick (Figure 3). The matrix is composed of arenite, calcarenite, and marly limestone. The tread of FT_6 terrace is found between 231 and 125 m of elevation a.s.l. and locally the FT_6 deposit is composed of gravel, 1–2 m thick. More detailed description and interpretations are made on the remaining FT_1, FT_2, FT_4, FT_5, and FT_7 fluvial terraces.

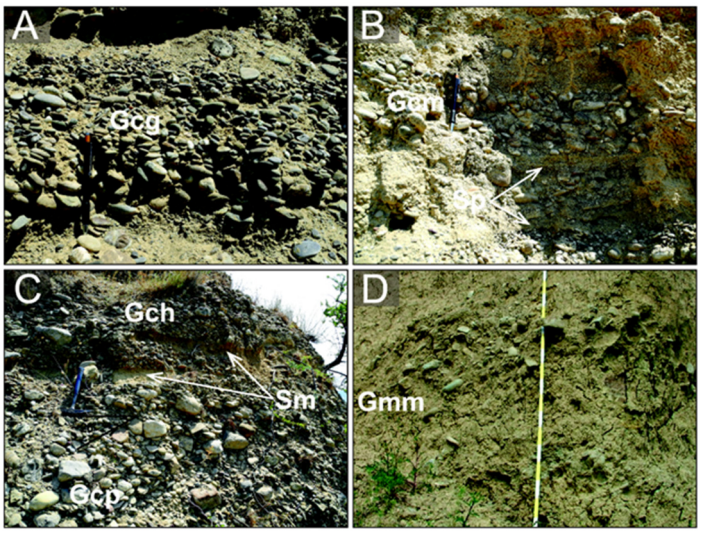

Figure 4. Photos showing the main gravelly facies (**A**, **B**, **C**, and **D**), with subordinate sandy facies (A, and C), recognized in the Pescogrosso fluvial catchment. For facies code and interpretation see Table 1.

*4.1. S. Maria d'Anglona Unit (**FT$_1$**)*

The FT_1 terraced deposit is located on the watershed of Agri and Sinni drainage basins, from 254 m to 260 m a.s.l., close to the Santa Maria d'Anglona church (Figure 3a). The FT_1 deposit rests on clayey bedrock (Argille subappennine *Auctt.*) younger than ~645 ky [67] pertaining to the Bradano Foredeep clastics sequence. It is formed of two fining upward depositional sequences, named as FT_{1a} and FT_{1b}, of ~18 m of thickness, overall. Moreover, the FT_1 deposit was displaced by a sin-sedimentary fault with vertical displacement of 40 cm (Figure 5). The FT_{1a} depositional sequence is composed of three distinct lithofacies separated by minor internal discontinuities. From bottom to top, it crops out the following deposits: (*i)* graded and clast-supported dark gravels, 1 m thick, clasts are sub-rounded and imbricated and are assembled in 7–20 cm thick layers (Gcg in Figure 5 and Table 1); (*ii)* massive and clast-supported dark gravel of 1.25 m thick organized in 10 cm thick layers (Gcm in Figure 5 and Table 1) with interbedded layers of coarse sand showing low-angle cross lamination (Sp in Figure 5 and Table 1); (*iii)* thin layers of sand, silt, and mud with locally ripple structures ~2 m thick (Fsl in Figure 5 and Table 1).

The FT_{1b} sequence is formed of clast-supported gravels, 8 m thick, with oblique layers dipping = 26° = east (Gcp in Figure 5 and Table 1); clasts are from rounded to sub-rounded and interbedding of massive middle-fine sands (Sm in Figure 5 and Table 1) are also present. The upper 5 m of the succession are composed of sand, silt, and mud with horizontal parallel lamination (Fsl in Table 1) and massive sandy layers (Sm in Table 1). Clasts of both the FT_{1a} and FT_{1b} sequences range from 1 to 10 cm of diameter and are composed of metamorphic rocks, sandstones, siltstones, and calcarenites. Only in the FT_{1b} are sub-rounded clasts found with 15–50 cm of diameter composed of sandstones and calcarenites. The FT_1 bed deposit shows clear evidence of fluvial processes as testified by the Gcm and Gcg deposits of the FT_{1a} sequence that could be attributed to debris flow (*sensu* [66]) e/o hyperconcentrated flows [68,69] occurred in fluvial systems. Enrichment of sand in the central portion of FT_1 sequence marks a shift to a sub-critical flow regime in the river, when a waning of high energy flows occurred. Gravels of the FT_{1b} bottom sequence are channelized and are interpreted as longitudinal (Gch in Figure 5 and Table 1) and/or lateral (Gcp in Figure 5 and Table 1) bars [66]. Moreover, fine sand, silt, and mud deposits of either the FT_{1a} and FT_{1b} sequences were assigned to overbank flows [66,70,71] or waning flows depositional facies. Considering the present-day nearness of the Ionian Sea, about 20 km far away, the different facies of the FT_{1a} and FT_{1b} sequences could be correlated with past sea-level variations and particularly to different highstands, following [14–17],

as discussed below. In particular, the FT_{1a} facies could be related to a coastal plain dominated by fluvial sedimentation during a highstand pulse of the Ionian sea level and the deposit sources, considering the shape, lithology, and good rounding of clasts, should be assigned to the denudation of both the older marine terraces and conglomerates units of the western Bradano Foredeep.

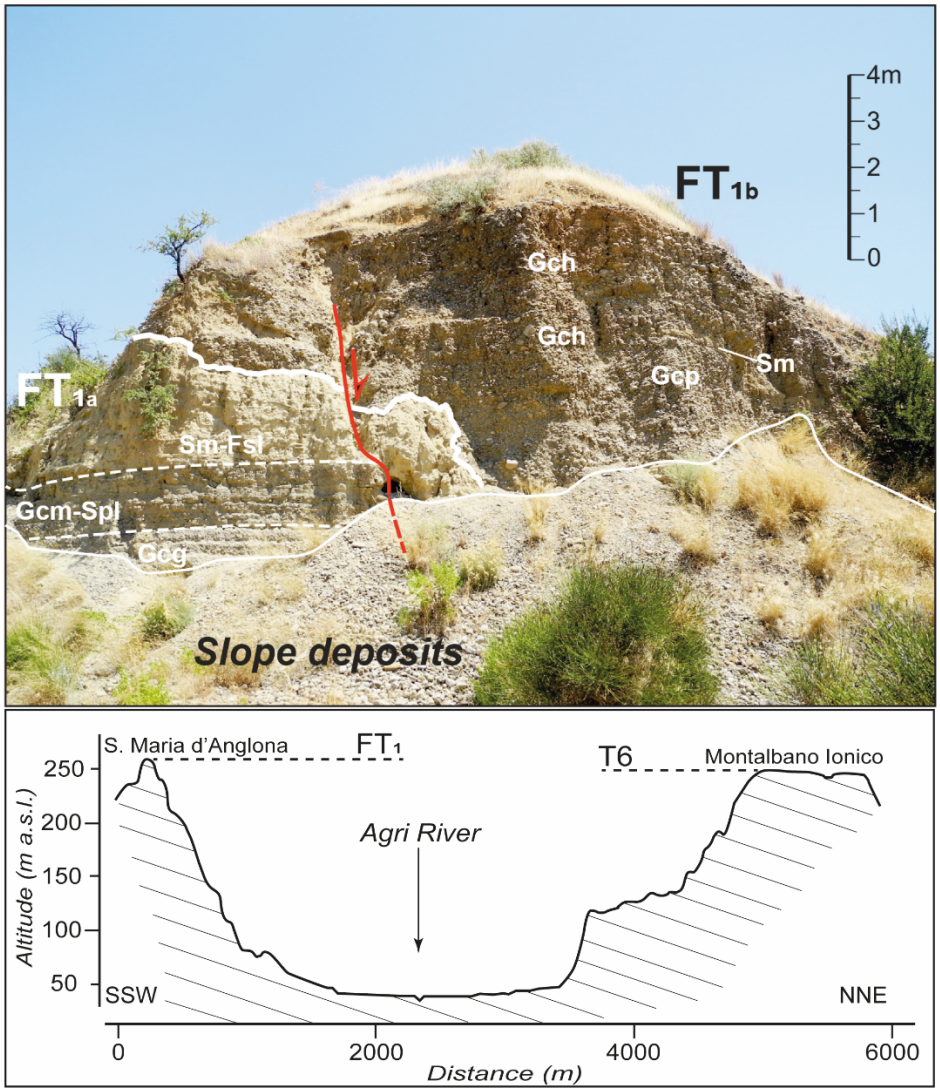

Figure 5. The photo shows both the FT_{1a} and FT_{1b} sedimentary sequences of the S. Maria d'Anglona unit separated by a minor internal discontinuity (coarse white line). White dashed line divides the two lithofacies. Red line marks the synsedimentary normal fault. See Table 1 for facies code and interpretation. The topographical cross-profile in the box below shows the altimetrical correspondence of the FT_1 fluvial terrace and the T6 marine terrace.

*4.2. Croce d'Anglona Unit (**FT_2**)*

The basal erosional surface of the FT_2 units carved into clayey bedrock is located between 202 and 245 m of altitude a.s.l., and dips east of ~1.3° (Figure 3a). The FT_2 deposit is composed of two sedimentary sequences, the lower (FT_{2a}) and the upper (FT_{2b}), separated by a minor internal discontinuity. The lower sequence, of about 5 m thick, is formed of clast-supported gravels (15 cm of max diameter) with mainly horizontal and trough cross lamination sets (Gch and Gct in Figure 6A and Table 1), and subordinately massive sets (Gcm in Figure 6A and Table 1). Upward, it passes to a middle-fine massive sands deposit (Sm in Figure 6A and Table 1) with interbedded silt and mud and showing a thin lamination (Fsl in Figure 6A and Table 1). The upper sequence, of about 3 m

thick, is entirely composed of massive and clast-supported gravels (30 cm of max diameter) (Gcm in Figure 6A and Table 1), forming superposed palaeochannels ranging from 1 to 3 m width. Both clast sequences are sub-rounded to rounded in shape and composed of arenaceous, calcarenite, and calcisitite metamorphic rocks of the Frido Fm. Dominance of massive sand sets in the lower sequence is related to hyperconentrated flows with fast deposition [69] during a fall of flow energy [72]. Subordinate gravel lenses (Gcm and Gch in Table 1) are related to inertial bedloads and turbolent flows [66] or alternatively to hyperconcentrated flows [68,69] assigned to longitudinal bars and/or sieve deposits [66]. Gravels of the Gct facies are assigned to channel transport events [66].

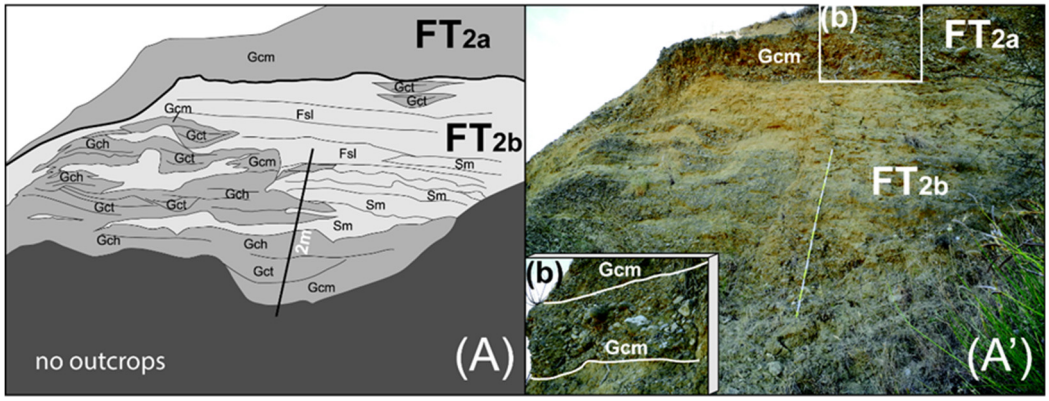

Figure 6. Depositional facies architecture of the Croce d'Anglona unit is shown in the cartoon (**A**) and in the field view (**A'**). The box (b) is a detail of the FT_2 upper sequence. See Table 1 for facies code and interpretation.

Upwards, the dominance of the Fsl facies shows episodes of overbank and waning in the channel system [66,70,71]. Conversely, the upper depositional sequence is mainly formed of gravels (Gcm in Table 1) reflecting debris flows facies that allowed a large tabular assemblage of gravel facies in a short vertical sedimentation space [73]. The sedimentary body of the FT_2 terrace could be referred to as a constructive alluvial plain mainly characterized by massive debris deposition.

*4.3. Cugno Longo Unit (**FT$_4$**)*

The Cugno Longo terrace is the first terrace placed within the present-day drainage basin of the Pescogrosso Stream. It is located on both the left-side and right-side interfluves of the catchment. Two terraces alignments are grouped within this unit: the first and most evident terrace alignment (FT_{4a}) is distributed near the left-side of the watershed from the Tursi Village to the Cugno Longo site, whereas the second and less evident (FT_{4b}) was distributed in the left-side valley of the Pescogrosso Stream (Figure 3). The basal erosional surface of the FT_{4a} deposit is located on the left-side valley and is elongated from NW to SE showing a concave upward surface with a lowest elevation of about 159 m a.s.l. at Fosso della Canala site (Figure 3). The surface rises of elevation at about 162 m a.s.l. toward southeast, and at about 300 m a.s.l. toward northwest close the Tursi Village, respectively. At Cugno Longo site, the FT_4 terrace deposit fills a 250–500 m-length palaeovalley, carved in the clayey bedrock. Moreover, the palaeovalley is ~120 m height, measuring from its bottom to the FT_1 tread surface. The whole thickness of the FT_4 terrace deposit varies from 10 m, at the Tursi Village, to 16.8 m, at the Fosso della Canala site and the infill shows a fining upward succession (Figure 7A).

The bed deposit is formed of massive clast-supported gravels from 3 to 4.5 m of thickness and the sand matrix is of medium–coarse size (Gcm in Figure 7B and Table 1). Sub-rounded to rounded clasts are of 40 cm max of diameter and are composed of arenites, calcarenite, calcisiltite, and calcareous breccias. Upwards, there are sets of medium-sized sand with horizontal lamination (Sh in Figure 7B and Table 1) and rarely massive sand (Sm in Figure 7B and Table 1). Close the S. Maria d'Anglona site and at about 8 m of height from its basal surface, the sand body is divided by a palaeosoil layer

1 m thick. It is important to note that within the sand and below the palaeosoil (Figure 7B), there are infrequent lenses 3–7 m width of clast- and matrix-supported massive gravel (Gcm facies). The FT_{4b} terraces found at the end of the Pescogrosso channel stream show a straight distribution, parallel to the present-day stream, and arranged from 232 m to 180 m of altitude a.s.l. (Figure 3). They represent relics of strath terraces and only sparse gravels are found in the field. The bottom coarse deposits of FT_{4a} sequence suggest a debris flow facies and then a palaeochannel with high energy flow and high stream power [66,68,69]. The clear passage to the upper sand body marks a variation toward a fluvial plain dominated by planar flows with critical regime indicating sheet flood facies [66] with intermittent episodes of coarse-grained debris flows. The increase of discharge flows is also marked by a decrease of their intensity upward. Finally, an absence of the fluvial activity is revealed by the palaeosoil (10^0–10^2 years, [74]).

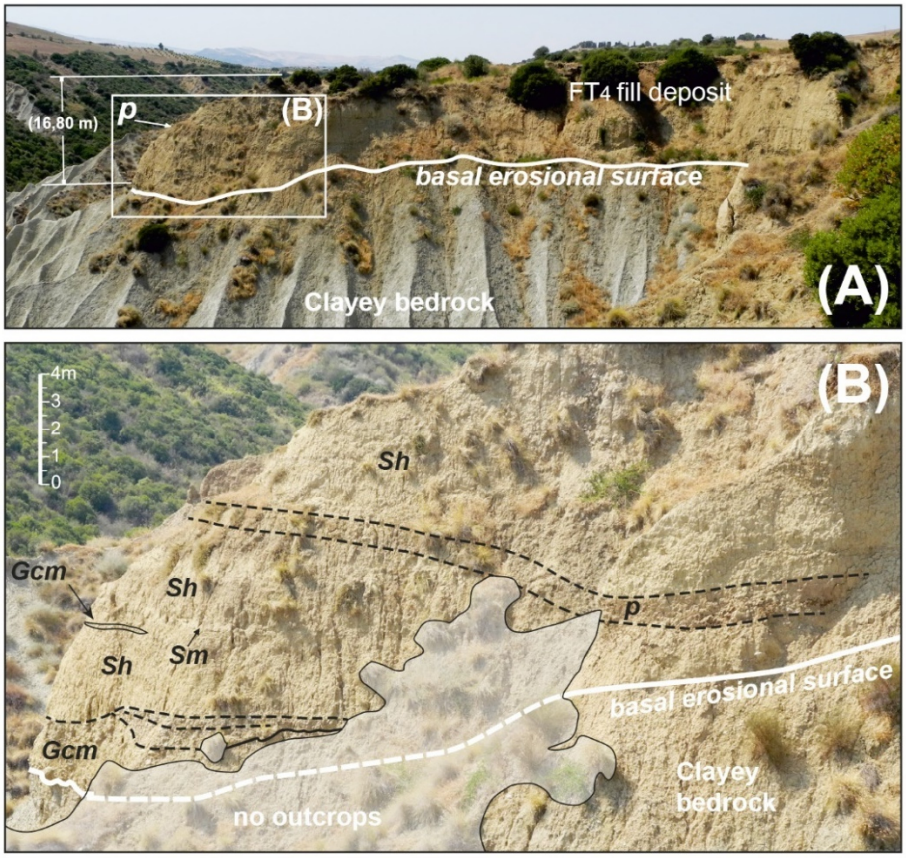

Figure 7. Panoramic view of the Cugno Longo terraced unit (**A**). In frame (**B**) is a detail of the FT_{4a} depositional facies architecture and the location of the palaeosoil (P). See Table 1 for facies code and interpretation.

*4.4. San Francesco Unit (**FT$_5$**)*

The San Francesco unit is found between 274 m and 224 m of elevation a.s.l. and is entirely included within the Pescogrosso catchment. The FT_5 fluvial deposit rests on Quaternary sands bedrock of the Bradano Foredeep and reaches ~15 m of thickness (Figure 8A). It is formed of a FT_{5a} lower unit and a FT_{5b} upper unit separated by a palaeosoil containing a thepra layer (Figure 8D). The FT_{5a} units is composed of two superposed fining upward sequences. From bottom to top there are massive clast-supported gravels (Gcm; Table 1) embedded in yellow-ocher sandy matrix and organized with decimeter to meter thick of amalgamated strata. The thickness of gravel sequence varies from 4.5 m to 3 m and the clast sizes are included into two range of 40–90 cm (Figure 8C), and 10–30 cm diameters, respectively. Upwards, there is a massive yellow sand sequence without sedimentary structures and from 3 to 1.6 m thick (Figure 8B).

On the top of this sandy sequence rests a brown sand palaeosoil (P in; Table 1), 60 cm thick, that seems to be weakly weathered because no well-developed horizons are visible. On the palaeosoil (P) rests a tephra layer (TU1, Figure 8A,D), composed of 12 cm thick of massive gray falling ash (Am in Table 1) covered by 39 cm thick of gray ash with cross lamination ripples (Ar in Table 1) and 60 cm thick of massive brown ash (Am in Table 1). Embedded within the latter ash strata there are sedimentary clasts of 1 to 10 cm of diameter. The FT_{5b} unit is formed of massive and clast-supported gravels (Gcm in Table 1) showing amalgamated layers, embedded in brown sandy matrix. The deposit is about 2 m thick; clasts are from rounded to sub-rounded, and are composed of limestone, marly limestone, sandstone, siltstone, and siliceous rocks. The gravelly sequence of FT_5 terraced deposit could be assigned to a fluvial plain facies dominated by pseudoplastic debris flow processes [66,68,69], while the sandy sequences could suggest a decrease of the flow energy and, as a consequence, a decrease of the sediment load and erosion. The upward decrease in size and the increase in roundness observed in the coarse gravels, placed at bottom of the FT_{5a} fluvial sequence (Figure 8C), could suggest a depositional process triggered by a tectonic event that produce a slope increase. Indeed, according to [20] a differential tectonic uplift was occurred in the backward Valsinni Ridge at this time. It is worth noting that this depositional sequence does not exclude different interpretations on the origin of the slope increase, such as the transition from a very distal to a more proximal floodplain position or to a change of discharge power.

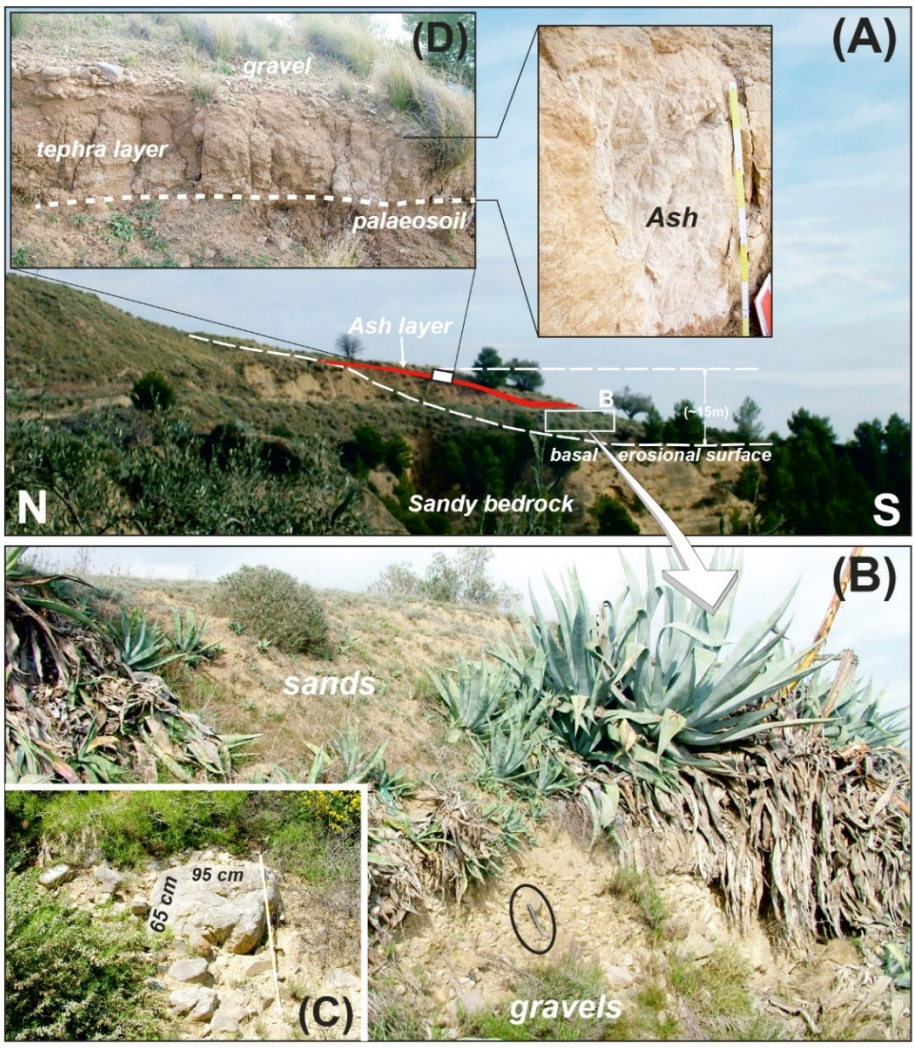

Figure 8. Panoramic view of the S. Francesco terraced unit (**A**). Fining upward sequence at the bottom of the FT_{5a} subunit (**B**). Coarse gravel embedded in the FT_{5a} deposit (**C**). The two small boxes in (A) show details of the tephra layer TU1 (**D**).

*4.5. San Teodoro Unit (**FT$_7$**)*

The FT_7 terraces are found in the surroundings of the Tursi Village, at ~225 m of elevation a.s.l. and at the mouth of Pescogrosso Stream, at ~116 m of elevation a.s.l. (Figure 3), respectively. They show deposits of 4.5 m thick, overall. Two distinct depositional sequences, the FT_{7a} and FT_{7b}, were recognized in the terraced deposits of the Tursi area (Figure 9A).

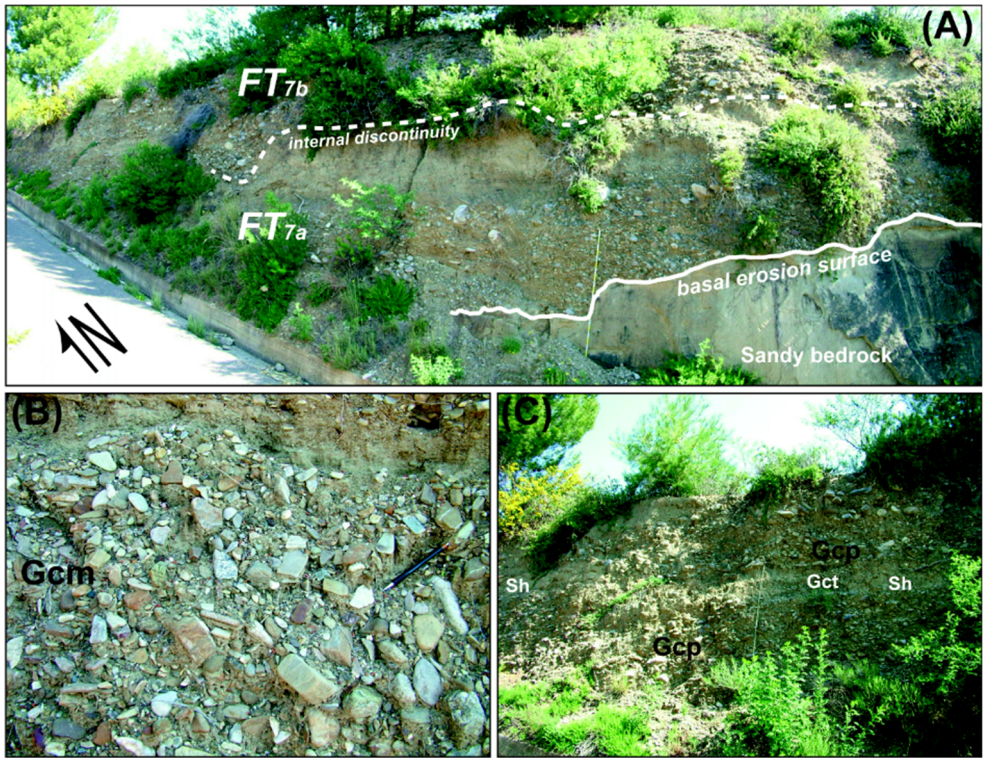

Figure 9. View of the two sedimentary sequences forming the S. Teodoro unit, close to the Tursi Village (**A**). Detail of the sub-angular pebbles assigned to the Gcm facies (**B**) and crops out of the FT_{7b} depositional sequence (**C**). See Table 1 for facies code and interpretation.

The FT_{7a} unit is composed of a fining upward sequence, formed at the bottom by ~4 m-thick gravel and passing upward to sand 1.4 m thick. The massive and clast-supported gravels form layers of tenses centimeters thick (Gcm in Figure 9B and Table 1), with interbedded middle-coarse sands with horizontal lamination (Sh in Table 1) increasing upward. Within the sandy levels thin-laminated clayey-silty layers (Fsl in Table 1) are interbedded and small bodies of horizontally aligned gravelly clasts (0.5–1 cm of diameter) are found. The FT_{7b} unit is formed of clast-supported gravels with planar cross stratification (Gcp in Figure 9C and Table 1) and middle-coarse sand with horizontal lamination (Sh; Table 1; Figure 13). Fine gravels with concave cross stratification (Gct in Figure 9C and Table 1) are also interbedded. Both the FT_{7a} and FT_{7b} deposits contain sub-angular and rarely sub-rounded clasts, composed of sandstones, calcarenites, siltites, and calcareous breccias (Figure 9B). The average diameter of clasts varies from 3 cm to 20 cm and rare blocks of ~40 cm at the bottom of the FT_{7a} sequence are also present. Near the Pescogrosso mouth, the FT_{7b} fluvial deposit is composed of horizontal stratified clast-supported gravels (Gch in Table 1). Upwards, there are lenses of middle sand with horizontal lamination (Sh in Table 1) and in the sedimentary top there are 1.1 m-thick poorly weathered silty sands (P in Table 1). The gravels outcropping between Ponte Masone and Sinni River sites could be attributed to supercritical regime flows forming longitudinal bars at the Pescogrosso mouth, and the sandy sequences interbedded to gravels could be assigned to sheet flood alluvial facies (*sensu* [66]). Fluvial features have been observed at the Tursi Village as follow: (i) low thickness than 5 m of the FT_7 deposits, (ii) width of the fluvial valley of ~570 m, (iii) erosional discontinuity between

the FT_{7a} and FT_{7b} units (Figure 9A), and (iv) dominance of sandy laminar flows (sh in Table 1) with interbedded overbank deposits (Fsl in Table 1) in the FT_{7b} sequence. All these features seem to be indicative of steady-state conditions in the fluvial vertical incision favoring the activation of lateral planation in the thalweg. Thus, the FT_{7a} sandy sequence could be interpreted as an abandonment channel deposit and the FT_{7b} minor internal discontinuity as a new channel bottom, laterally shifted (Figure 9A). The analysis of the gravelly deposits outcropping at Tursi Village and the morphology of the FT_{7b} discontinuity allowed the assignment of the FT_{7a} deposits to a proximal alluvial fan controlled by debris flow processes [66,68,69], and the upward FT_{7b} deposits to an intermediate alluvial fan. The overlap of facies from the intermediate to the proximal fan indicates a decrease of the sediment supply produced by a decrease of the stream power probably generated by a lowering of the channel slope gradient climatically induced in the catchment basin.

4.6. Tephra Layer Analysis and Interpretation

The FT_{5a} and FT_{5b} depositional sequences of the S. Francesco unit are separated by a tephra layer (TU1 in Figure 10) about 1 m thick that rests on the palaeosoil P (Figure 8). The chemical analysis of the tephra ash (TU1) was realized at the DST of the University of Pisa by means of an electronic microscope. The sampled ash is composed of well-vesciculated micropumice including pyroclastic glasses a few microns thick (Figure 10). The glass is clear and there are no microcrystals in the matrix. The Energy Dispersive Spectrometers (EDS) chemical analyses allowed us to classify the glass by means of the Total Alkali Silica (TAS) classification diagram as trachytes if samples also fall at the bound of the Phonolites field (Figure 10). Glass composition is quite homogeneous for the most analyzed chemical elements and is divided in two groups based on the alkali ratio contain (Table 2). Comparison of the TU1 ash, based on ESD data, with many tephra compositions made in the Europe area has shown a good correspondence of lithological and geochemical characters between the TU1 and the X-6 tephra pertained to the magmatic Campanian Province [75]. Table 3 shows the TU1 geochemical analyses are well fitted to datasets from the scientific literature concerning the X-6 tephra in both the central Mediterranean area and Balcanian chain [75–79]. Moreover, the absolute age of the X-6 tephra obtained by the $^{40}Ar/^{39}Ar$ radiometric technique was of 107 ± 2 ka BP [80], which fits very well to the absolute age of 10,843 ka computed from varve deposit counting in the Lago Grande di Monticchio [78].

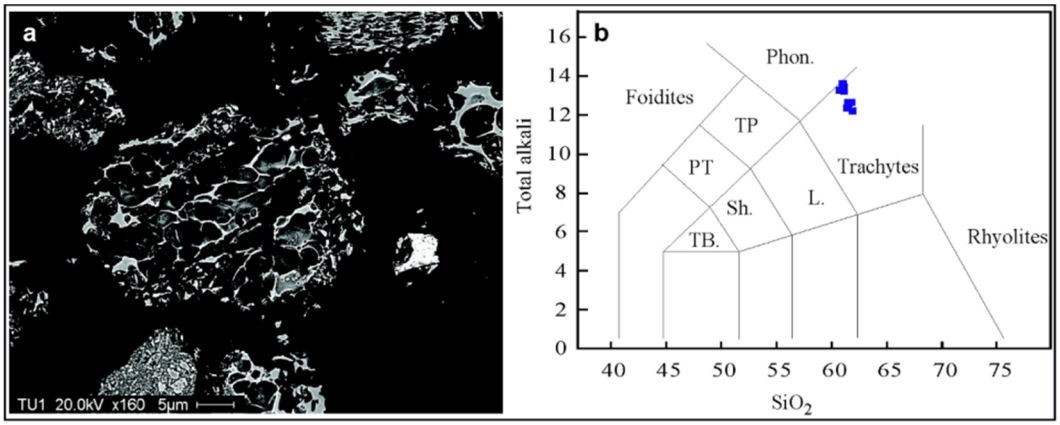

Figure 10. Electronic microscope photo of the ash clasts sampled in the TU1 tephra (**a**). TAS classification diagram of the EDS ash composition (**b**).

Table 2. EDS chemical analysis of the tephra samples TU1. s.d.: Standard deviation.

	1	**2**	**5**	**8**	**9**	**11**	**12**	**3**	**4**	**6**	**7**	**10**	**Av. 1**	**s.d.**	**Av. 2**	**s.d.**
SiO_2	60.93	61.09	61.13	60.98	61.15	60.74	61.04	61.87	61.51	61.47	61.39	61.75	61.01	0.14	61.60	0.20
TiO2	0.47	0.44	0.43	0.41	0.54	0.61	0.49	0.58	0.52	0.52	0.57	0.41	0.48	0.07	0.52	0.07
Al_2O_3	18.86	18.74	18.92	18.74	18.86	18.95	18.92	19.07	18.89	18.94	18.85	19.09	18.86	0.09	18.97	0.11
FeOtot	3.15	3.05	3.1	3.18	2.93	3.12	3.07	3.16	3.25	3.02	3.29	3.1	3.09	0.08	3.16	0.11
MnO	0.29	0.24	0.29	0.37	0.25	0.36	0.29	0.35	0.39	0.45	0.46	0.18	0.30	0.05	0.37	0.11
MgO	0.45	0.48	0.36	0.27	0.42	0.37	0.41	0.34	0.34	0.42	0.31	0.25	0.39	0.07	0.33	0.06
CaO	1.69	1.71	1.69	1.54	1.68	1.73	1.55	1.68	1.63	1.69	1.85	1.77	1.66	0.08	1.72	0.09
Na_2O	6.68	6.75	6.53	6.74	6.51	6.74	6.94	5.55	5.85	5.88	5,.66	5.98	6.70	0.15	5.78	0.17
K_2O	6.61	6.7	6.71	6.91	6.87	6.55	6.5	6.67	6.78	6.79	6.72	6.7	6.69	0.15	6.73	0.05
P_2O_5	0	0	0	0	0	0	0	0	0	0	0	0	0.00	0.00	0.00	0.00
ClO	0.87	0.8	0.84	0.86	0.79	0.83	0.8	0.73	0.82	0.83	0.9	0.77	0.83	0.03	0.81	0.06
Total	100	100	100	100	100	100	100.01	100	99.98	100.01	100	100				
tot. alk.	13.29	13.45	13.24	13.65	13.38	13.29	13.44	12.22	12.63	12.67	12.38	12.68				
Alk.ratio	0.99	0.99	1.03	1.03	1.06	0.97	0.94	1.20	1.16	1.15	1.19	1.12				

Table 3. Comparison among the EDS data related to the ash sample TU1 and the X-6 tephra composition of the Central Mediterranean. The references of X-6 tephra are as follows: OT0702-9 by Vogel et al. (2010) [79], TM27 by Wulf et al. (2008) [78], S10 by Munno et al. (2007) [77], KET8004-975 by Paterne et al. (1988) [76]. s.d.: Standard deviation, n.a.: not available.

	TU1a	**s.d.**	**TU1b**	**s.d.**	**OT0702-9a**	**s.d.**	**OT0702-9b**	**s.d.**	**TM27a**	**s.d.**	**TM27b**	**s.d.**	**S10**	**s.d.**	**KET8004-975**
SiO_2	61.01	0.14	61.60	0.20	60.97	0.25	61.42	0.19	60.79	0.33	61.56	0.18	62.38	0.39	62.38
TiO_2	0.48	0.07	0.52	0.07	0.46	0.07	0.47	0.07	0.48	0.03	0.45	0.02	0.40	0.08	0.33
Al_2O_3	18.86	0.09	18.97	0.11	18.83	0.12	18.80	0.14	18.55	0.10	18.52	0.07	18.86	0.17	18.72
FeO_{tot}	3.09	0.08	3.16	0.11	3.14	0.14	3.00	0.11	2.98	0.11	2.78	0.08	2.81	0.30	2.68
MnO	0.30	0.05	0.37	0.11	0.32	0.09	0.24	0.08	0.31	0.03	0.20	0.02	0.24	0.08	n.a.
MgO	0.39	0.07	0.33	0.06	0.33	0.05	0.50	0.07	0.30	0.01	0.45	0.05	0.29	0.10	0.1
CaO	1.66	0.08	1.72	0.09	1.65	0.10	1.71	0.04	1.73	0.06	1.89	0.08	1.61	0.10	1.85
Na_2O	6.70	0.15	5.78	0.17	6.84	0.27	5.70	0.30	7.21	0.28	5.88	0.19	6.02	0.46	6.66
K_2O	6.69	0.15	6.73	0.05	6.66	0.18	7.60	0.24	6.54	0.16	7.57	0.18	7.39	0.55	7.27
P_2O_5	0.00	0.00	0.00	0,00	0.00	0.00	0.00	0.00	0.04	0.03	0.08	0.04	n.a.	-	n.a.
ClO	0.83	0.03	0.81	0.06	0.80	0.06	0.56	0.08	0.89	0.08	0.63	0.07	n.a.	-	n.a.
Total	100.00		100.00		100.00		100.00		99.82		100.00		100.00		99.99
tot. alk.	13.39		12.52		13.50		13.30		13.75		13.45		13.41		13.93
alk.ratio	1.00		1.16		0.97		1.33		0.91		1.29		1.23		1.09

4.7. Analysis of Terraces Longitudinal Profile

The longitudinal profile of fluvial terraces outcropping in the study area has been carried out and its elevation a.s.l. has been plotted against the present-day Pescogrosso Stream (Figures 11 and 12) thus recognizing eight terrace orders. The three higher and older are those found at Santa Maria d'Anglona site, out of the Pescogrosso drainage basin and are the FT_1, FT_2, and FT_3 fluvial terraces, whereas the five lower and younger terraces are found within the drainage basin and are those from FT_4 to FT_8 (Figures 3, 11 and 12). It is worth noting that the FT_4 terrace is the only landform outcropping in both the Santa Maria d'Anglona site and the Pescogrosso basin, and allowed us to correlate these two groups of terraces. It is well known that among factors in controlling the slope and the arrangement of longitudinal terrace profiles [14,20,81] there are: (i) variations of the base level; (ii) regional and local tectonic uplift; (iii) climate changes; and (iv) heterogeneity of geological substrate or catchment size. These factors produce significant slope gradients variations in the fluvial longitudinal profiles, allowing us to interpret them as climate-induced or tectonically induced landforms. FT_1, FT_2, and FT_3 terraces are placed on the watershed of the Pescogrosso catchment that partially corresponds to the left-side divide of the Sinni drainage basin (and correspondingly to the right-side divide of the Agri drainage basin; see Figure 3 for details). The eastward-dipping slope gradient of the FT_1 and FT_2 profiles is almost the same and then they are parallel downstream, while that of the FT_3 shows an increase of the slope gradient producing a diverging downstream profile [20,81] (Figure 13). The FT_4 is the first fluvial terrace profile located within the Pescogrosso catchment and then its base level will be obviously referred to the mouth of the Pescogrosso Stream in the Sinni River that differs from the previous FT_1, FT_2, and FT_3 terraces base level. Moreover, the lower slope gradient of the FT_4 terrace than the older terraces, as observed in the longitudinal profiles (Figure 12), also demonstrate such a difference. The basal erosional discontinuity of the FT_4 deposit shows a complex concave upward geometry given by a knickpoint and two points of fluvial capture (Figure 13) placed at the Ponte Masone and Fosso della Canala sites.

Its longitudinal profile plotted against the FT_3 profile shows a lower slope gradient (Figures 12 and 13) than the FT_3. The different altitude observed between the FT_3 and FT_4 local base levels could be attributed to their different mouths related to the Ionian Sea and the Sinni River, respectively. This means that the different base levels could be responsible for their converging downstream longitudinal profiles (Figure 13). Consequently, this latter geometry seems not to be related to tectonic activity of the backward Valsinni Ridge. The basal surfaces of the FT_5, FT_6, and FT_7 fluvial terraces show similar longitudinal profiles than the FT_4 because of the same base level related to the Sinni River was there. Moreover, these latter terraces show two concave upward inflection points and a knickpoint such as the FT_4 (Figure 13) to reinforce this interpretation. We observe that knickpoints and inflection points are placed at the same position in the diagram and all longitudinal slope profiles are converging downstream. Only the inflection points from FT_5 to FT_7 shows a decreasing in slope (Figure 13). Considering FT_6, FT_7, and FT_8 as paired terraces, it is possible to measure their palaeovalley widths, which are 815 m (FT_6), 570 m (FT_7), and 290 m (FT_8). As a result, the decrease in width from the old (FT_6) to young (FT_8) terraces has occurred. The analysis of longitudinal profiles has shown a complex architecture of terraces mainly controlled by different base levels of erosion. Consequently, the base level of FT_1, FT_2, and FT_3 terraces would seem to have been the Ionian Sea, while that of FT_4, FT_5, FT_6, and FT_7 terraces the Sinni River.

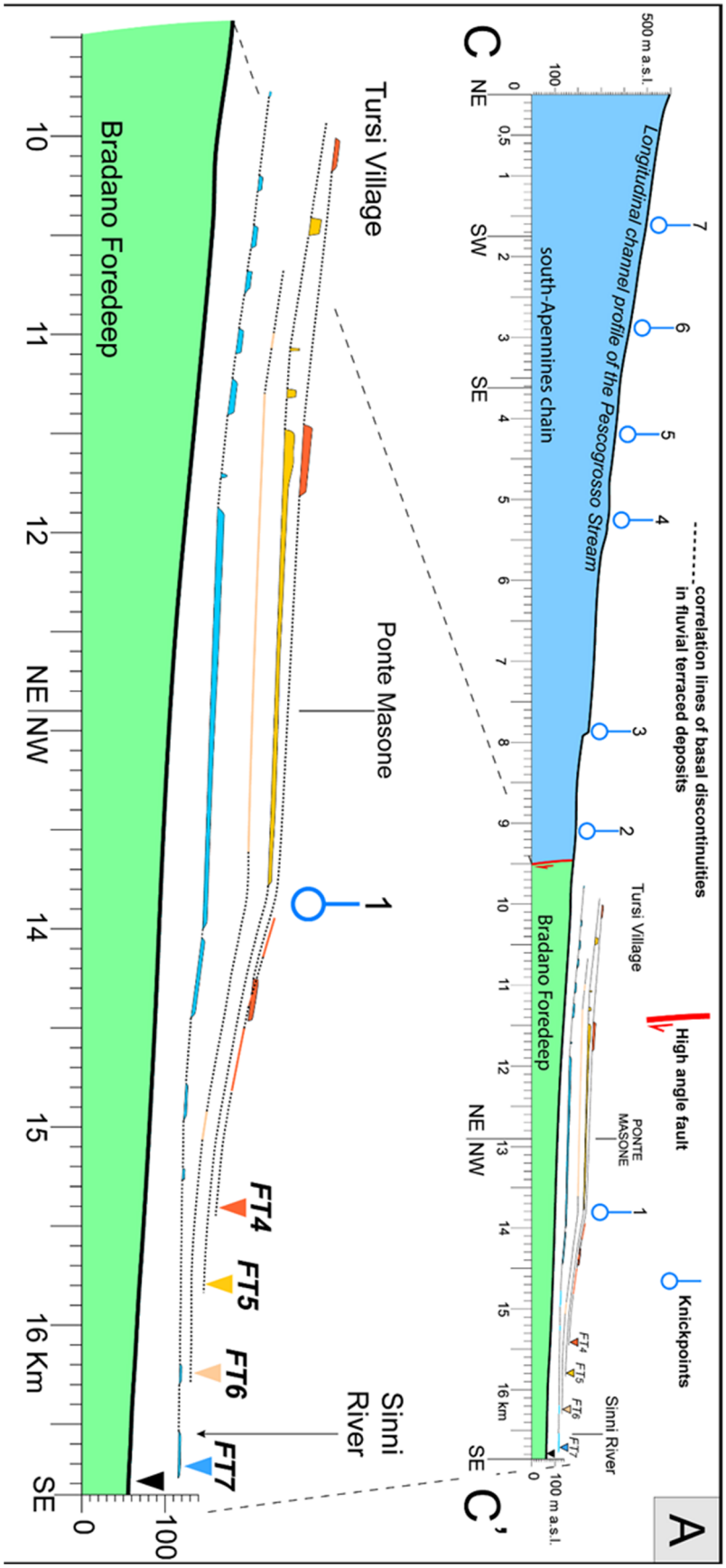

Figure 11. Plot of the longitudinal terrace profiles against the present-day Pescogrosso channel profile. See text for explanations and Figure 3 for profile location.

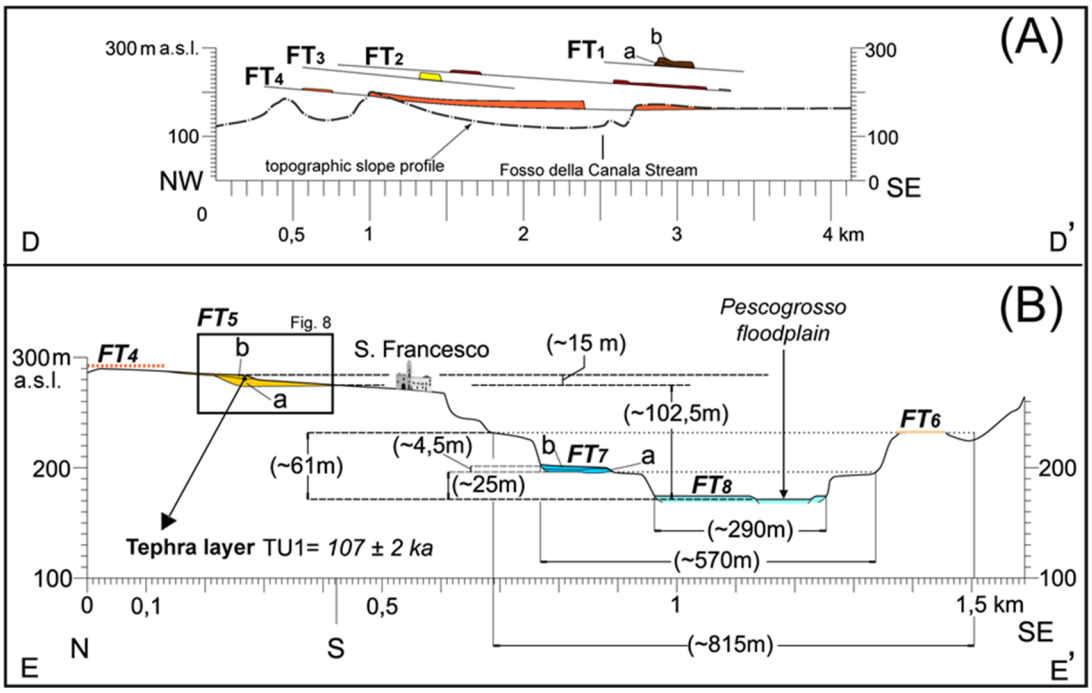

Figure 12. Plot of fluvial terraces against the topographic slope profile of the Cugno Longo hanging valley (**A**). Transverse topographic profile of the Pescogrosso Stream valley and location of the fluvial terraces (**B**). See Figure 3 for location of the trace profile.

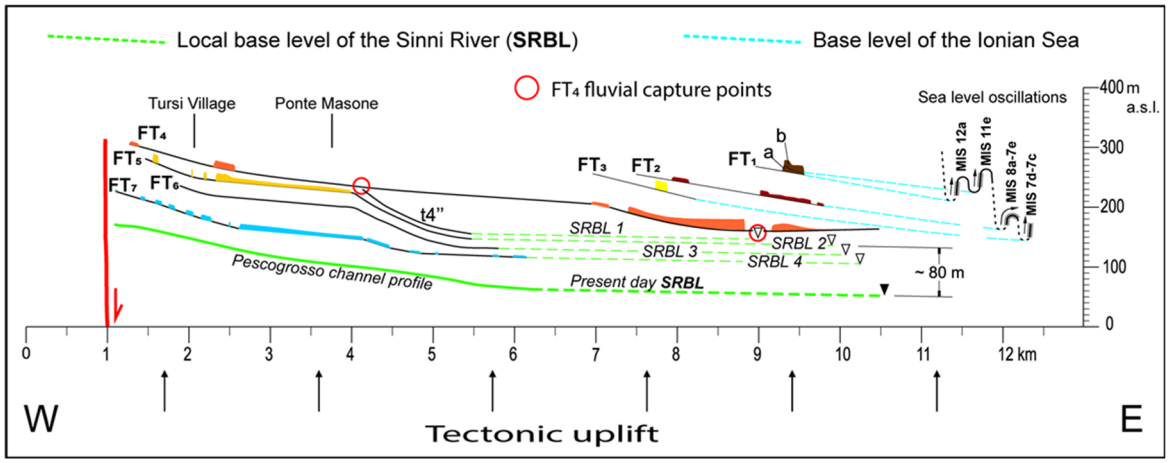

Figure 13. Plot of fluvial terraces profiles and correlation with the regional base level, corresponding to the Ionian Sea, and the local base level, corresponding to the Sinni River. It is also shown as the FT_1, FT_2, and FT_3 terraces were influenced by highstand/lowstand oscillation of the Ionian sea level within the MIS variations.

5. Discussion

5.1. Relationships among Fluvial Terraces, Sea-Level Changes, Climate, and Tectonics

As shown in the previous sections, two main groups of fluvial terraces are found in the Pescogrosso catchment and surrounding areas. The first group is formed by the older terraces FT_1, FT_2, and FT_3, distributed close to the Pescogrosso watershed. The second group is composed of the younger terraces named as FT_4, FT_5, FT_6, FT_7, and FT_8 which are distributed within the Pescogrosso drainage basin (Figure 3). The oldest and highest fluvial terrace is found at the Santa Maria d'Anglona (FT_1 unit) and is distributed on the watershed dividing the Agri and Sinni drainage basins, between 260 and 250 m

of altitude a.s.l. (Figure 3). The geomorphological correlation of the FT_1 fluvial terrace and the T6 Ionian marine terrace attributed to MIS13 [27,49–54] in the marine isotope oxygen curve (Figure 14) allowed us to obtain the absolute age of the FT_1 terrace. It is worth noting that the T6 marine terrace is located at the Montalbano Ionico site, in the left-side valley of the Agri drainage basin (Figure 2a) at about 5 km far away from the FT_1 terrace (Figure 5). According to Ciaranfi et al. (2010) [67] the sedimentary top of the T6 marine terrace is composed of conglomerates with red sandy-clayey matrix, a few meters thick, pertaining to fluvial environment. It is worth noting that the marine deposit of the T6 terrace was assigned by Sauber et al. (2010) [52] to MIS13 and the subsequent fluvial aggradation must be likely assigned to MIS12. A similar consideration was reached by Westaway and Bridgland (2007) [27] that assigned to MIS14 or 12 the gravel sequence of fluvial deposits capping the T6 marine terrace. They follow the assumption that fluvial aggradation was recorded during a cold climate stage corresponding to cold episode in the marine isotopic stages. The same elevation, ranging from 260 to 250 m a.s.l., was measured on both the FT_1 fluvial terrace, at the S. Maria d'Anglona site, and the T6 marine terrace, at the Montalbano site (Figure 5). Therefore, the morphological closeness of these two terraces, as already observed by [52] and the analogy of their depositional facies, allowed us to correlate their depositional fluvial sequence. It occurred during the episode of fluvial plain aggradation that produced the sedimentary top of the T6 marine terrace. Accordingly, the attribution of the FT_1 fluvial deposit of Santa Maria d'Anglona to the transition from MIS12 to MIS11 (*sensu* [15]) seems to be reliable. This is in good agreement with the interpretation of the T6 marine terrace realized by Westaway and Bridgland (2007) [27]. In such a way, the fluvial episodes responsible for the FT_1 unit formation could be related to a same base level and then to a same coastal-fluvial plain connected to the palaeoshore line of the Ionian Sea. Moreover, plotting the MIS stages of FT_1 deposits in the diagram of the marine oxygen isotope curve [82] (Figure 14), has been possible to extract its absolute age that ranging from 440 to 420 ka, corresponding to the cold to warm transition from MIS12 to MIS11.

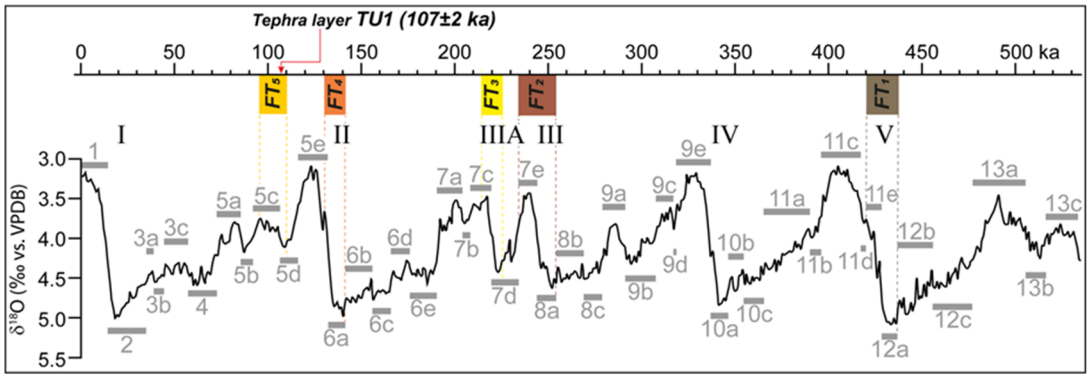

Figure 14. Diagram of the Marine Isotope Oxygen Stages for the last 500 ka (modified after [82]) showing the proposed age of formation of the studied fluvial terraces based on correlations with marine terraces. Red line indicates the chronological position of the TU1 tephra layer in the FT_5 terraced unit.

The closeness of the Ionian Sea coastal plain, about 20 km away, suggested we should include the study area in the frame of an incised-valley system produced by fluvial incision and influenced by the drop and rise of the relative sea level (*sensu* [14]). Consequently, the sequence-stratigraphic concepts, following [15–17], have been attempted to be applied for the older FT_1, FT_2, and FT_3 fluvial terraces. As stated above, the minor internal discontinuity between the FT_{1a} and FT_{1b} sub-units was preliminary assigned to a lowstand stage of the sea level that triggered the vertical fluvial incision and the valley deepening in a subaerial coastal plain [15,83,84]. During this time, the vertical incision of the Pescogrosso palaeostream produced an enlargement of its drainage basin upwards, eroding the bedrock of the Valsinni Ridge anticline. This backward process explains the increase of the clast diameter and the decrease of their roundness in the FT_{1b} sequence—that is mainly formed by rocks coming from the Valsinni Ridge—regarding the FT_{1a}. Finally, the filling of the fluvial palaeovalley

was realized by the FT_{1b} sequence during the subsequent sea-level rise, as reported in the eustatic sea-level curve (MIS11e; Figure 14). Near the FT_1 unit crops out the younger FT_2 terraced deposit of the Croce d'Anglona unit (Figure 3) which represents the infill of a fluvial palaeovalley, about 65 m deep and distributed from 202 to 245 m of altitude a.s.l. which was built in the clayey bedrock of the Bradano Foredeep.

At about 2 km length eastwards, there is the T5 marine terrace of the Ionian Sea, attributed to the whole MIS9 [52,54] which crops out at ~210 m a.s.l. The well-fitting morphological correlation of FT_2 terraces (Figures 2 and 11) and T5 marine terrace allowed us to refer the FT_2 deposit to the cold to warm transition of the MIS8a. This means that fluvial deposition was partially controlled by the Ionian sea-level variations, as already recognized in the older FT_1 terrace. Consequently, the assemblage of depositional bodies in the lower sequence reflects a sedimentation controlled by the raising of the sea level (transgressive system tract *sensu* [83]) that has been tentatively assigned to MIS8a (Figure 14). In a similar way, the facies arrangement of the upper sequence is linked to the following steady state of the sea level or highstand system tract *sensu* [83]. This latter was related to the subsequent interglacial sub-stage corresponding to MIS7e (Figure 14). Therefore, the increase of the clast shape and the increase of the sediment supply in the FT_2 deposit could be attributed to climate variations. Unfortunately, little information is available for the FT_3 terraced deposit and thus it has only been possible to realize its longitudinal slope profile. The good morphological correspondence with the older FT_1 and FT_2 terrace profiles allowed us to link its evolution and base-level variation to these latter. In a frame of stratigraphic continuity with the older terraces, we have tentatively correlated the deposition of the FT_3 terraced unit to the transition from cold to warm of the sub-stages MIS7d/MIS7c (Figure 14).

The alignment from west to east (from the Tursi Village to the S. Maria d'Anglona) of the FT_{4a} strath terraces suggests a palaeochannel flowing toward the Ionian Sea that is here named the Cugno Long palaeostream (Figure 3). The absence of stratigraphic details in the FT_{4b} terraced deposit does not allow interpretation of their depositional facies. From a morphological point of view, we observe that FT_{4b} terraces profile alignment is developed along a N-S-oriented straight-line, quite perpendicular to the Sinni River profiles and shows a slope of about 3–4° (Figures 11 and 12). This field observation allowed us to recognize a fluvial elbow in the Cugno Longo palaeostream that was produced by a fluvial capture process by a tributary of the Sinni River. As stated above, the difference in slope gradient of FT_3 and FT_4 terrace profiles, together with the fluvial elbow in the Cugno Longo valley and its piracy seems to be good an indicator of a base level corresponding to the Sinni River, and not to the Ionian Sea (see Figure 13). Focusing on the previous reasoning and considering: (a) the morphological continuity between the FT_3 and FT_4, and (b) the time needs for the fluvial capture of the Cugno Longo palaeostream by the Sinni River, we have tentatively placed the FT_4 terraced deposit in the MIS6a stage, younger than the FT_3 (Figure 14). This attribution fits well with the Piano Codicino fluvial terrace, assigned to MIS6 at about 130 ka [20,27]. The terrace is located backwards of the Valsinni Ridge and out of the studied area. It is found within the Sinni River drainage basin from 420 to 305 m of elevation a.s.l. and shows a height on the Sinni thalweg of 113 ± 2 m [20]. Considering the highest altitude of the FT_4 terrace as close to the Tursi Village at about 300 m of elevation a.s.l. and the lowest one of the Piano Codicino terrace at about 305 m a.s.l. seems to be reliable a morphological correlation between these two end points. The Piano Codicino strath terrace was carved on a wide floodplain in the Sant'Arcangelo Basin and was connected through the Valsinni gorge to the FT_4 Cugno Longo terrace thus to suggests that the morphological threshold of Valsinni Ridge anticline was already partially formed during the MIS6. In such a way, the FT_4 terrace could represents the lower reach of the Piano Codicino palaeostream placed out of the Sant'Arcangelo Basin and within the morphological apex of the Bradano Foredeep area. Accordingly, it was tectonically raised after the aggradation of the Piano Codicino fluvial deposit dated to ~130 ka [20,27]. In fact, the differential uplift occurred after ~130 ka triggered the backward incision by the Sinni River in the Valsinni Ridge thus to complete the incision of the present-day gorge river valley. The sedimentary variation in the FT_{5a} fining upward sequence is correlated with climate changes that occurred before the deposition of

the tephra layer TU1 assigned at 107 ± 2 ka BP by geochemical correlation with the X-6 tephra of the magmatic Campanian Province [75]. Therefore, the sedimentary variation could be referred to as the MIS5d and MIS5c stages (Figure 14). Before the TU1 tephra fall, a warm climate occurred in the area as suggested by the red palaeosoil (P) outcropping below. The unconformity between the FT_{5a} and FT_{5b} sequences seems to be produced by a large mass movement that blocked the sediment supply thus forming an ephemeral lacustrine area, subsequently incised by fluvial erosion. This interpretation is supported by well-developed lacustrine deposits recognized within the Pescogrosso channel that pass upward to epiclastic sediments composed of volcanic debris and ash flows.

5.2. Geomorphological Evolution of the Pescogrosso Catchment Area

The development of fluvial terraces in the Pescogrosso catchment area allowed discrimination of the role played by climate and tectonics in their formation and evolution. These geomorphological variations have been summarized into three different evolutionary stages (Figure 15). The first stage (Figure 15A) was related to the formation of FT_1, FT_2, and FT_3 fluvial terraces. They are composed of gravels and sands deposits 18 m (FT_1), 8 m (FT_2), and 15 m (FT_3) thick, respectively, and represent the remnants of floodplains flowing toward east and which were linked to different past base levels of the Ionian Sea (Figure 15A). It is worth noting that during this time, the Ionian palaeoshoreline was shifted east, because of the regional uplift. At the same time, the glacioeustatic oscillations of the sea level induced by climatic change in response to astronomical force variations were responsible for the deposition of FT_{1a}, FT_{1b} sub-units, and FT_2 and FT_3 units. The FT_{1a} and FT_{1b} sequences attributed to two different depositional facies show clear variation in the stratigrahical organization. This allowed correlation of the two depositional sequences to relative highstands of the sea level corresponding to the MIS12a and MIS11e sub-stages (Figure 14) following the model proposed by [14]. In particular, the FT_{1a} facies could be related to a coastal plain dominated by fluvial sedimentation in a highstand pulse of the sea level during MIS12a (Figure 14). Indeed, considering the shape, lithology, and good rounding of clasts of FT_{1a} deposits, it could be possible to infer their origin from the denudation of older marine terraces and conglomerate units of the western side of Bradano Foredeep. If it is true, then it is possible to suppose that the FT_1 palaeostream flowed on the Quaternary clastics of the Bradano Foredeep and not on the Apennines Unit deposits. The minor internal discontinuity dividing FT_{1a} and FT_{1b} deposits could be assigned to a lowstand of the MIS12a (Figure 14). Such a lowstand triggered the vertical fluvial incision and the valley deepening in the subaerial coastal plain. During the whole phase of evolution, the upward fluvial incision of the Pescogrosso palaeostream produced the enlargement of its drainage basin that reaches up the Apennines unit bedrock of the Valsinni Ridge. The backward erosional process could justify the increase of the clast diameter and the decrease of their roundness in the FT_{1b} deposit (it is mainly formed by rocks of the Valsinni Ridge) regarding the FT_{1a} one. Finally, the FT_{1b} sequence represents the palaeovalley infill that occurred in the subsequent sea-level rise, as reported in the eustatic sea-level curve (MIS11e; Figure 14). With the same reasoning it is possible to associate both the FT_2 and FT_3 sequences to the base level of the Ionian Sea.

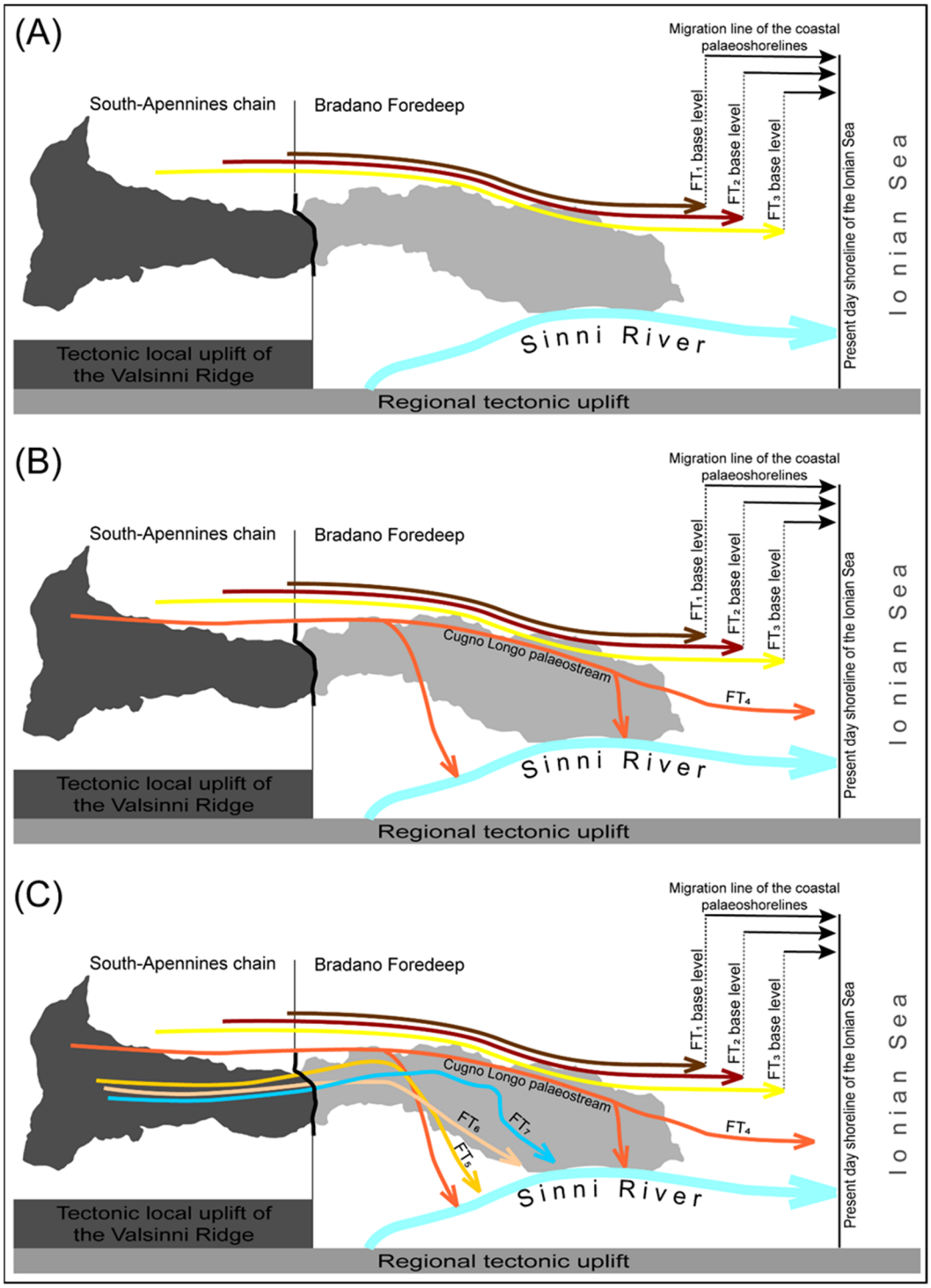

Figure 15. Sketch map of the three evolutionary stages (**A**, **B**, and **C**) in the formation and evolution of the fluvial terraces in the Pescogrosso drainage basin and surrounding areas. See text for explanation.

The second stage (Figure 15B) occurred during the formation of the Cugno Longo palaeostream and is shown by the FT_4 terraced deposit, about 10–16.8 m thick. The FT_4 terraced deposit is included in the second group of lower and younger terraces and represents the first terraces pertained to the Pescogrosso catchment stream (Figures 3 and 11). The terrace alignments that form the FT_4 units are developed from west to east, suggesting a palaeochannel direction oriented toward the Ionian Sea, named as Cugno Long palaeostream. Conversely, the FT_{4b} tread terraces alignment are distributed along a N-S-oriented straight line, sloping by about 3–4° (Figures 3 and 11), perpendicular to the Sinni

River direction. This abrupt diversion of the FT_{4a} and FT_{4b} terraces alignment suggests a piracy of the Cugno Longo palaeostream by the Fosso della Canala Stream, a tributary of the Sinni River (Figures 3 and 12). The fluvial capture leads to a change of local base level, from the Ionian Sea (FT_{4a} terraces) to the Sinni River (FT_{4b} terraces) and consequently to a variation in the input factors in controlling the facies formation. Glacioeustatic variation of Ionian sea level in the FT_{4a} sequence and climate and tectonics activities in the FT_{4b} terraces might be the factors in controlling the intensity, frequency, sediment load, and shape and roundness of clasts in the two terraces. The lower part of the FT_{4a} sequence is formed by massive and clast-supported gravel assigned to debris flow facies characterizing a channel with high energy flow and high stream power (see Section 4.3). It has been attributed to a dry climate with low rainfalls with concentrated and isolated torrential events. Conversely, the upper sandy facies suggest a variation toward a fluvial plain dominated by sheet flood facies (see Section 4.3) that could be attributed to a wet climate with rainfall well distributed during the seasons and a decrease of the extreme pluvial events. The alignment east of the Cugno Longo palaeostream was the same as the three older streams and, moreover, two points of fluvial capture are found along its longitudinal profile, at Fosso della Canala and Ponte Masone sites (Figure 13), respectively. The piracy probably happened in different times, first at Fosso della Canala and after at Ponte Masone by means of two left-tributary streams of the Sinni River oriented about NNW-SSE and indicated as t4′ and t4″ segments in the fluvial terrace profile (Figures 13 and 15).

The third stage (Figure 15C) started with the formation of the FT_5 terrace, ~15 m thick, and marks the more recent geomorphological evolution of the Pescogrosso Stream valley. The fluvial sequences in this stage are constrained by the absolute age of 107 ± 2 ka BP of the TU1 tephra layer sampled in the FT_5 subunit and was assigned to MIS5d-5c (Figure 14). However, the terrace development is also controlled by tectonic activity affecting the backward area of the Valsinni Ridge. The coarse-grained clasts recognized in the bottom of the FT_{5b} subunit that attain about 95 cm of diameter (Figure 8C) are completely absent in both the older and younger terraced deposits and they could be attributed to a higher slope gradient profile. This sedimentological evidence is in good agreement with the unconformity placed between the FT_4 and FT_5 terraced deposits showing a slope decrease of the bottom surface between Tursi Village and Ponte Masone sites (Figure 13). These variations in the slope gradient might be indicative of a local uplift (*sensu* [20,81]) that occurred in the Valsinni Ridge, as already recognized by Giano and Giannandrea (2014) and by Gioia et al. (2018) [20,46]. The two younger FT_6 and FT_7 terraces show deposits less than 5 m thick and their distribution allowed us to assign them as strath terraces [15]. Considering that the drainage valley of the Pescogrosso Stram is mainly composed of sand and clay deposits pertaining to the Bradano Foredeep, a computation of the bedrock incision rate equal to ~1.2 mm/year has been carried out. The value is measured starting from the age of the FT_5 sedimentary top, extracted by the MIS5c curve and corresponding to ~98 ka (Figure 14), and from the present-day thalweg altitude a.s.l. of 117.7 m measured in the Pescogrosso Stream (Figure 12B). Furthermore, the width of the FT_6 and FT_7 palaeofloodplains, ranging from ~815 m to ~570 m, together with the sedimentological features of the FT_7 terraced deposit, suggest a decrease in the vertical incision during the terrace formation that favors lateral planation processes. This is well shown in the NW-SE-oriented reach of the Pescogrosso fluvial valley, based on the progressive eastward migration of the terraces from FT_4 to FT_7 (Figure 15). The progressive eastward migration of the terrace profile, the vertical incision rates of 1.25 mm/year in the last 125 ka and of ~0.9 mm/year in the last 2 Ma [26], the same location of the FT_4, FT_5, FT_6, and FT_7 knickpoints in the longitudinal terrace profiles, are good indicators of a superimposition of the local uplift on the regional one. The local uplift can be attributed to the activity of the frontal thrust belt buried below the Quaternary clastic deposits of the Bradano Foredeep. The frontal thrust belt was responsible for a re-activation of high-angle faults in the Valsinni Ridge close to the Sinni River that controlled the evolution of the Pescogrosso fluvial valley. Moreover, the FT_4 and FT_5 sedimentary sequences show temporary interruption in the fluvial deposition caused by large landslides that dammed the Pescogrosso valley. Consequently, a small lacustrine environment was created thus to break off the sediment load in the Pescogrosso channel.

6. Conclusions

The location of the Pescogrosso small fluvial catchment together with the well-exposed and developed Quaternary fluvial terraces allowed partial recognition of the contribution furnished by local and regional tectonic uplift, climate change, and base-level oscillations in the geomorphological evolution of the area. The comparison of detailed facies analysis of fluvial depositional sequences, the morphological interpretation of longitudinal terrace profiles, the dating of a tephra layer interbedded in the FT_5 fluvial terrace, and the location and age of both the T6 and T5 marine terraces are the main tools used in this research. Finally, the application of the sequence-stratigraphic concepts to depositional fluvial units has furnished more details on the Pescogrosso incised-valley system. Two groups of fluvial terraces have been differentiated: the first and older is composed of three FT_1, FT_2, and FT_3 units which were strictly influenced by the drop and rise of the Ionian sea level; the second group is formed by the younger terraces listed from the FT_4 to the FT_7 controlled by the local base level of the Sinni River valley. Three evolutionary stages affecting the study area have been detected (Figure 15). The first (Figure 15A) was responsible for the formation of the FT_1, FT_2, and FT_3 fluvial units. These units pertain to an incised-valley system produced by fluvial incision and influenced by the drop and rise of the relative level of the Ionian Sea. Applying both the sequence-stratigraphic concepts on fluvial deposits and the geomorphological analysis, the three fluvial terraces have been correlated with the T6 and T5 marine terraces of the Ionian area and then plotted in the MIS curve of [82] (Figure 1). The second stage (Figure 15B) was characterized by the formation and the development of the FT_4 units. The terrace distribution allowed identification of the Cugno Longo palaeostream. The latter firstly moved toward the Ionian Sea and then was captured by the Sinni River shifting its flow direction by about 90° (Figure 15B). Consequently, a clear fluvial elbow was formed. The third stage (Figure 15C) started with the FT_5 terraced deposit containing the tephra layer TU1 interbedded in the fluvial unit. The absolute age of the tephra permitted us to exactly date the FT_5 unit at 107 ± 2 ky. Moreover, this age has been plotted in the marine isotope oxygen curve (Figure 14). The morphological evolution of the study area continues with the evolution of the younger fluvial terraces, indicating a decrease in the vertical fluvial incision and an increase in the lateral planation processes in response to a slowdown of the local and regional tectonic uplift. The formation and development of the eight fluvial terraces in the Pescogrosso catchment and surrounding areas was certainly controlled by the Ionian sea-level glacioeustatic variations in association with the Middle and Late Pleistocene regional uplift of the Apennine chain [26,27], affecting the whole Ionian arc. In fact, it is already demonstrated that the rates of the tectonic uplift in marine terraces of southern Ionian arc are distributed in a range of 1.25–0.18 mm/year during the last 125 ky. Furthermore, the analysis of the right-angle pattern of minor fluvial network in the whole Metaponto area has revealed the development of the Ionian hydrographic network. It has been attributed to a bending of the Bradano Foredeep area due to the propagation toward both the east-northeast and south-east of blind thrusting of the "Campano-Lucano" and Calabrian segments of the southern Apennines chain [29,46].

Author Contributions: Conceptualization, P.G. and S.I.G.; methodology, P.G. and S.I.G.; software, P.G., S.I.G., and R.S.; validation, P.G., S.I.G., and R.S.; formal analysis, P.G.; investigation, P.G.; resources, P.G., S.I.G.; data curation, P.G:, S.I.G., and R.S.; writing—original draft preparation, S.I.G.; writing—review and editing, S.I.G.; supervision, P.G. and S.I.G.

Funding: This research was funded by Università della Basilicata RIL 2015 and FFABR, granted at S.I. Giano.

Acknowledgments: We are thanks the three anonymous referees which greatly contributed in the improvement of the original manuscript. A special thanks to the Guest Editor M. Lazzari for its critical suggestions.

Conflicts of Interest: The authors declare no conflict of interest.

References

1. Stokes, M.; Cunha, P.P.; Martins, A.A. Techniques for analysing Late Cenozoic river terrace sequences. *Geomorphology* **2012**, *165–166*, 1–6. [CrossRef]

2. Blum, M.D.; Törnqvist, T.E. Fluvial response to climate and sea-level change: A review and look forward. *Sedimentology* **2000**, *47*, 2–48. [CrossRef]
3. Bridgland, D.R.; Westaway, R. Climatically controlled river terrace staircases: A worldwide Quaternary phenomenon. *Geomorphology* **2008**, *98*, 285–315. [CrossRef]
4. Finnegan, N.J.; Roe, G.; Montgomery, D.R.; Hallet, B. Controls on the channel width of rivers: Implications for modeling fluvial incision of bedrock. *Geology* **2005**, *33*, 229–232. [CrossRef]
5. Garcia, A.F.; Mahan, S.A. The notion of climate-driven strath-terrace production assessed via dissimilar stream-processes response to late Quaternary climate. *Geomorphology* **2014**, *214*, 223–244. [CrossRef]
6. Gibbard, P.L.; Lewin, J. River incision and terrace formation in the Late Cenozioc of Europe. *Tectonophysics* **2009**, *474*, 41–55. [CrossRef]
7. Hancock, G.S.; Anderson, R.S. Numerical modeling of fluvial strath-terrace formation in response to oscillating climate. *Geol. Soc. Am. Bull.* **2002**, *114*, 1131–1142.
8. Hartshorn, K.; Hovius, N.; Dade, W.B.; Slingerland, R.L. Climate-drivenbedrockincision in an active mountain belt. *Science* **2002**, *397*, 2036–2038. [CrossRef]
9. Macklin, M.G.; Fuller, I.C.; Lewin, J.; Maas, G.S.; Passmore, D.G.; Rose, J.; Woodward, J.C.; Black, S.; Hamlin, R.H.B.; Rowan, J.S. Correlation of fluvial sequences in the Mediterranean basin over the last 200 ka and their relationship to climate change. *Quat. Sci. Rev.* **2002**, *21*, 1633–1641. [CrossRef]
10. Merritts, D.J.; Vincent, K.R.; Wohl, E.E. Long river profiles, tectonism, and eustasy: A guide to interpreting fluvial terraces. *J. Geophys. Res.* **1994**, *99*, 14031–14050. [CrossRef]
11. Pazzaglia, F.J.; Brandon, M.T. A fluvial record of long-term steady-state uplift and erosion across the Cascadia forearc high, Western Washington State. *Am. J. Sci.* **2001**, *301*, 385–431. [CrossRef]
12. Starkel, L. Climatically controlled terraces in uplifting mountain areas. *Quat. Sci. Rev.* **2003**, *22*, 2189–2198. [CrossRef]
13. Vandenberghe, J. The fluvial cycle at cold–warm–cold transitions in lowland regions: A refinement of theory. *Geomorphology* **2008**, *98*, 275–284. [CrossRef]
14. Zaitlin, B.A.; Dalrymple, R.W.; Boyd, R. The stratigraphic organization of incised-valley systems associated with relative sea-level change. In *Incised-valley System: Origin and Sedimentary Sequences*; Dalrymple, R.W., Boyd, R., Zaitlin, B.A., Eds.; SEPM Society for Sedimentary Geology: Tulsa, OK, USA, 1994; vol. 51, pp. 45–60.
15. Van Wagoner, J.; Posamentier, H.W.; Mitchum, R.M.; Vail, P.R.; Sarg, J.F.; Loutit, T.S.; Hardenbol, J. An overview of the fundamentals of sequence stratigraphy and key definitions. *Soc. Econ. Paleo. Miner.* **1988**, *42*, 39–45.
16. Van Wagoner, J.C.; Mitchum, R.M.; Campion, K.M.; Rahmanian, V.D. Siliciclastic sequence stratigraphy in well logs, cores, and outcrops: Concepts for high-resolution correlation of time and facies. *AAPG Methods Explor. Ser.* **1990**, *7*, 55.
17. Vail, P.R.; Audemar, F.; Bowman, S.A.; Einser, P.N.; Perez-Cruz, C. The stratigraphic signatures of tectonic, eustasy and sedimentology: An overview. In *Cycles and Events in Stratigraphy*; Einsele, G., Ricken, W., Seilacher, A., Eds.; Springer Verlag: Berlin, Germany, 1991; pp. 617–659.
18. Cyr, A.J.; Granger, D.E. Dynamic equilibrium among erosion, river incision, and coastal uplift in the Northern and Central Apennines, Italy. *Geology* **2008**, *36*, 103–106. [CrossRef]
19. D'Agostino, N.; Jackson, J.A.; Dramis, F.; Funiciello, R. Interactions between mantle upwelling, drainage evolution and active normal faulting: An example from the central Apennines (Italy). *Geophys. J. Int.* **2001**, *147*, 475–497. [CrossRef]
20. Giano, S.I.; Giannandrea, P. Late pleistocene differential uplift inferred from the analysis of fluvial terraces (Southern Apennines, Italy). *Geomorphology* **2014**, *217*, 89–105. [CrossRef]
21. Nesci, O.; Savelli, D.; Troiani, F. Late Quaternary alluvial fans in the northern Marche Apennines: Implications of climate changes. *Alp. Meditarranean Quat. (Il Quaternario)* **2010**, *23*, 146–156.
22. Troiani, F.; Della Seta, M. Geomorphological response of fluvial and coastal terraces to Quaternary tectonics and climate as revealed by geostatistical topographic analysis. *Earth Surf. Process. Landf.* **2011**, *36*, 1193–1208. [CrossRef]
23. Vannoli, P.; Basili, R.; Valensise, G. New geomorphic evidence for anticlinal growth driven by blind-thrust faulting along the northern Marche coastal belt (central Italy). *J. Seismol.* **2004**, *8*, 297–312. [CrossRef]
24. Wegmann, K.W.; Pazzaglia, F.J. Late Quaternary fluvial terraces of the Romagna and Marche Apennines, Italy: Climatic, lithologic, and tectonic controls on terrace genesis in an active orogen. *Quat. Sci. Rev.* **2009**, *28*, 137–165. [CrossRef]

25. Aringoli, D.; Cavitolo, P.; Farabollini, P.; Galindo-Zaldivar, J.; Gentili, B.; Giano, S.I.; Lòpez-Garrido, A.C.; Materazzi, M.; Nibbi, L.; Pedrera, A.; et al. Morphotectonic characterization of the Quaternary intermontane basins of the Umbria-Marche Apennines (Italy). *Rend. Fis. Acc. Lincei* **2014**, *25*, 111–128. [CrossRef]
26. Schiattarella, M.; Di Leo, P.; Beneduce, P.; Giano, S.I.; Martino, C. Tectonically driven exhumation of a young orogen: An example from southern Apennines, Italy. In *Tectonics, Climate, and Landscape Evolution*; Willett, S.D., Hovius, N., Brandon, M.T., Fisher, D., Eds.; Special Paper 398, Penrose Conference Series; The Geological Society of America: Boulder, CO, USA, 2006; Volume 398, pp. 371–385.
27. Westaway, R.; Bridgland, D. Late Cenozoic uplift of southern Italy deduced from fluvial and marine sediments: Coupling between surface processes and lower-crustal flow. *Quat. Int.* **2007**, *175*, 86–124. [CrossRef]
28. Schiattarella, M.; Giano, S.I.; Gioia, D.; Martino, C.; Nico, G. Age and statistical properties of the summit palaeosurface of southern Italy. *Geogr. Fis. Din. Quat.* **2013**, *36*, 289–302.
29. Giano, S.I.; Mecca, L.; Pascale, S.; Schiattarella, M. Morphometric analysis of the thrust front of the Lucanian Apennine, southern Italy. *Geogr. Fis. Din. Quat.* **2018**, *41*, 67–81.
30. Patacca, E.; Scandone, P. Geology of the Southern Apennines. *Boll. Soc. Geol. Ital.* **2007**, *7*, 75–119.
31. Beneduce, P.; Giano, S.I. Osservazioni preliminari sull'assetto morfostrutturale dell'edificio vulcanico del Monte Vulture (Basilicata). *Alp. Meditarranean Quat. (Il Quaternario)* **1996**, *9*, 325–330.
32. Pieri, P.; Vitale, G.; Beneduce, P.; Doglioni, C.; Gallicchio, S.; Giano, S.I.; Loizzo, R.; Moretti, M.; Prosser, G.; Sabato, L.; et al. Tettonica quaternaria dell'area Bradanico-Ionica. *Alp. Meditarranean Quat. (Il Quaternario)* **1997**, *10*, 535–542.
33. Barchi, M.R.; Amato, A.; Cippitelli, G.; Merlini, S.; Montone, P. Extensional tectonics and seismicity in the axial zone of the Southern Apennines. *Boll. Soc. Geol. Ital. (Ital. J. Geosci)* **2007**, *7*, 47–56.
34. Bavusi, M.; Chianese, D.; Giano, S.I.; Mucciarelli, M. Mustidisciplinary investigations on the Roman acqueduct of Grumentum (Basilicata, Southern Italy). *Ann. Geophys.* **2004**, *47*, 1791–1801.
35. Cinque, A.; Patacca, E.; Scandone, P.; Tozzi, M. Quaternary kinematic evolution of the Southern Apennines. Relationships between surface geological features and deep lithospheric structures. *Ann. Geophys.* **1993**, *36*, 249–260.
36. Giano, S.I. Quaternary alluvial fan systems of the Agri intermontane basin (southern Italy): Tectonic and climatic controls. *Geol. Carpath.* **2011**, *62*, 65–76. [CrossRef]
37. Giano, S.I.; Maschio, L.; Alessio, M.; Ferranti, L.; Improta, S.; Schiattarella, M. Radiocarbon dating of active faulting in the Agri high valley, Southern Italy. *J. Geodyn.* **2000**, *29*, 371–386. [CrossRef]
38. Giano, S.I.; Pescatore, E.; Agosta, F.; Prosssser, G. Geomorphic evidence of Quaternary tectonics within an underlap fault zone of southern Apennines, Italy. *Geomorphology* **2018**, *303*, 172–190. [CrossRef]
39. Schiattarella, M.; Giano, S.I.; Gioia, D. Long-term geomorphological evolution of the axial zone of the Campania-Lucania Apennine, Southern Italy: A review. *Geol. Carpath.* **2017**, *68*, 57–67. [CrossRef]
40. Ogniben, L. Schema introduttivo alla geologia del confine calabro-lucano. *Mem. Soc. Geol. It.* **1969**, *8*, 453–763.
41. Pescatore, T.; Renda, P.; Schiattarella, M.; Tramutoli, M. Stratigraphic and structural relationships between Meso-Cenozoic Lagonegro basin and coeval carbonate platforms in southern Apennines, Italy. *Tectonophysics* **1999**, *315*, 269–286. [CrossRef]
42. Di Leo, P.; Giano, S.I.; Gioia, D.; Mattei, M.; Pescatore, E.; Schiattarella, M. Evoluzione morfotettonica quaternaria del bacino intermontano di Sanza (Appennino meridionale). *Alp. Meditarranean Quat. (Il Quaternario)* **2009**, *22*, 189–206.
43. Giano, S.I. Geomorphology of the Agri intermontane basin (Val d'Agri-Lagonegrese National Park, Southern Italy). *J. Maps* **2016**, *12*, 639–648. [CrossRef]
44. Giano, S.I.; Schiattarella, M. Age constraints and denudation rate of a multistage fault line scarp: An example from southern Italy. *Geochronometria* **2014**, *41*, 245–255. [CrossRef]
45. Giano, S.I.; Gioia, D.; Schiattarella, M. Morphotectonic evolution of connected intermontane basins from the southern Apennines, Italy: The legacy of the pre-existing structurally controlled landscape. *Rend. Fis. Acc. Linc.* **2014**, *25*, 241–252. [CrossRef]
46. Gioia, D.; Schiattarella, M.; Giano, S.I. Right-Angle Pattern of Minor Fluvial Networks from the Ionian Terraced Belt, Southern Italy: Passive Structural Control or Foreland Bending? *Geosciences* **2018**, *8*, 331. [CrossRef]
47. Casnedi, R. La fossa bradanica: Origine, sedimentazione e migrazione. *Mem. Soc. Geol. It.* **1988**, *41*, 439–448.

48. Lazzari, M.; Pieri, P. Modello stratigrafico-deposizionale della successione regressiva infrapleistocenica della Fossa bradanica nell'area compresa tra Lavello, Genzano e Spinazzola. *Mem. Soc. Geol. It.* **2002**, *57*, 231–237.
49. Lazzari, M. Il comportamento tettonico e sedimentario del bacino d'avanfossa Bradanica durante il Pleistocene inferiore. *Mem. Descr. Carta Geol. It.* **2008**, *87*, 61–76.
50. Pieri, P.; Tropeano, M.; Sabato, L.; Lazzari, M.; Moretti, M. Quadro stratigrafico dei depositi regressivi della Fossa bradanica (Pleistocene) nell'area compresa fra Venosa e il Mar Ionio. *Giornale di Geologia* **1998**, *60*, 318–320.
51. Amato, A.; Dimase, A.C. Caratteristiche paleoambientali ed evoluzione geomorfologica dei plateaux della media valle del Fiume Agri (Basilicata). *Alp. Meditarranean Quat. (Il Quaternario)* **1997**, *10*, 213–230.
52. Brückner, H. Ausmaβ von Erosion und Akkumulation im Verlauf des Quartärs in der Basilicata (Süditalien). *Z. Geomorphol.* **1982**, *43*, 121–137.
53. Caputo, R.; Bianca, M.; D'Onofrio, R. Ionian marine terraces of southern Italy: Insights into the Quaternary tectonic evolution of the area. *Tectonics* **2010**, *29*. [CrossRef]
54. Cilumbriello, A.; Tropeano, M.; Sabato, L. The Quaternary terraced marine-deposits of the Metaponto area (Southern Italy) in a sequence-stratigraphic perspective. *Geoacta* **2008**, *1*, 29–54.
55. Sauber, D.; Wagner, S.; Brückner, H.; Scarciglia, F.; Mastronuzzi, G. Soil development on marine terraces near Metaponto (Gulf of Taranto, Southern Italy). *Quat. Int.* **2010**, *222*, 48–63.
56. De Santis, V.; Caldara, M.; Torres, T.; Ortiz, J.E.; Sanchez-Palencia, Y. A review of MIS 7 and MIS 5 terrace deposits along the Gulf of Taranto based on new stratigraphic and chronological data. *Ital. J. Geosci.* **2018**, *137*, 349–368. [CrossRef]
57. Bentivenga, M.; Coltorti, M.; Prosser, G.; Tavarnelli, E. A new interpretation of terraces in the Taranto Gulf: The role of extensional faulting. *Geomorphology* **2004**, *60*, 383–402. [CrossRef]
58. Zander, A.; Fülling, M.A.; Brückner, H.; Mastronuzzi, G. OSL dating of Upper Pleistocene littoral sediments: A contribution to the chronostratigraphy of raised marine terraces bordering the Gulf of Taranto, South Italy. *Geogr. Fis. Din. Quat.* **2006**, *29*, 33–50.
59. Calabrò, R.A.; Feltre, L.; Perotti, C.R. Structural features of the S. Arcangelo piggyback Basin (Southern Apennines, Italy) from seismic data and analogue modelling. *Boll. Soc. Geol. It.* **2002**, *1*, 333–341.
60. Turco, E.; Maresca, R.; Cappadona, P. La tettonica Plio-Pleistocenica del confine calabro-lucano: Modello cinematico. *Mem. Soc. Geol. It.* **1992**, *45*, 519–529.
61. Benvenuti, M.; Bonini, M.; Moratti, G.; Sani, F. Tectono sedimentary evolution of the Plio-Pleistocene Sant'Arcangelo Basin (Southern Apennines, Italy). In *Tectonics of the Western Mediterranean and North Africa*; Moratti, G., Chalouan, A., Eds.; Geological Society of London: London, UK, 2006; Volume 262, pp. 289–322.
62. Hippolyte, J.C.; Angelier, J.; Roure, F.; Casero, P. Piggyback basin development and thrust belt evolution: Structural and palaeostress analyses of Plio-Quaternary basins in the Southern Apennines. *J. Struct. Geol.* **1994**, *16*, 159–173. [CrossRef]
63. Pieri, P.; Sabato, L.; Loiacono, F.; Marino, M. Il bacino di piggyback di Sant'Arcangelo: Evoluzione tettonico-sedimentaria. *Boll. Soc. Geol. It.* **1994**, *113*, 468–481.
64. Mattei, M.; Petrocelli, V.; Lacava, D.; Schiattarella, M. Geodynamic implications of Pleistocene ultrarapid vertical-axis rotations in the Southern Apennines, Italy. *Geology* **1994**, *32*, 789–792. [CrossRef]
65. NASC (North American Commission on Stratigraphic Nomenclature). North American stratigraphic code. *Bull. Am. Assoc. Pet. Geol.* **1983**, *67*, 841–875.
66. Miall, A.D. *The Geology of Fluvial Deposits*; Springer Verlag: Berlin, Germany, 1996; pp. 1–502.
67. Ciaranfi, N.; Lirer, F.; Lirer, L.; Lourens, L.J.; Maiorano, P.; Marino, M.; Petrosino, P.; Sprovieri, M.; Stefanelli, S.; Brilli, M.; et al. Integrated stratigraphy and astronomical tuning of Lower–Middle Pleistocene Montalbano Jonico land section (Southern Italy). *Quat. Int.* **2010**, *219*, 109–120. [CrossRef]
68. Pierson, T.C. Erosion and deposition by debris flows at Mt. Thomas, north Canterbury, New Zealand. *Earth Surf. Proc. Land.* **1980**, *5*, 227–247. [CrossRef]
69. Smith, G.A. Coarse-grained non-marine volcaniclastic sediment: Terminology and depositional process. *Geol. Soc. Am. Bull.* **1986**, *97*, 1–10. [CrossRef]
70. Van Houten, F.B. Iron oxides in red beds. *Geol. Soc. Am. Bull.* **1986**, *79*, 917–920. [CrossRef]
71. Walker, T.R. Color of recent sediments in tropical Mexico: A contribution to the origin of red beds. *Geol. Soc. Am. Bull.* **1967**, *78*, 917–920. [CrossRef]

72. Dreyer, T. Quantified fluvial architecture in ephemeral stream deposits of the Esplugafreda Formation (Paleocene), Tremp-Graus basin, northern Spain. *Int. Ass. Sedim.* **1993**, *17*, 337–362. [CrossRef]
73. Heller, P.L.; Paola, C. The large-scale dynamics of grain-size variation in alluvional basins, 2: Application to syntectonic conglomerate. *Bas. Res.* **1992**, *4*, 91–102. [CrossRef]
74. Mack, G.H.; Madoff, R.D. A test of models of fluvial architecture in palaeosol development: Camp Rice Formation (Upper Pliocene–Lower Pleistocene) southern Rio Grande rift, New Mexico, USA. *Sedimentology* **2005**, *52*, 191–211. [CrossRef]
75. Keller, J.; Ryan, W.B.F.; Ninkovich, D.; Altherr, R. Explosive volcanic activity in the Mediterranean over the past 200,000 yr as recorded in deep-sea sediments. *Geol. Soc-Am. Bull.* **1978**, *89*, 591–604. [CrossRef]
76. Paterne, M.; Guichard, F.; Labeyrie, J. Explosive activity of the South Italian volcanoes during the past 80,000 years as determined by marine tephrochronology. *J. Volc. Geoth. Res.* **1988**, *34*, 153–172. [CrossRef]
77. Munno, R.; Petrosino, P. The late Quaternary tephrostratigraphical record of the San Gregorio Magno basin (southern Italy). *J. Quat. Sci.* **2007**, *22*, 247–266. [CrossRef]
78. Wulf, S.; Kraml, M.; Keller, J. Towards a detailed distal tephrostratigraphy in the Central Mediterranean: The last 20,000 yrs record of Lago Grande di Monticchio. *J. Volc. Geoth. Res.* **2008**, *177*, 118–132. [CrossRef]
79. Vogel, H.; Zanchetta, G.; Sulpizio, R.; Wagner, B.; Nowaczyk, N. A tephrostratigraphic record for the last glacial–interglacial cycle from Lake Ohrid, Albania and Macedonia. *J. Quat. Sci.* **2010**, *25*, 320–338. [CrossRef]
80. Brauer, A.; Allen, J.R.M.; Mingram, J.; Dulski, P.; Wulf, S.; Huntley, B. Evidence for the last interglacial chronology and environmental change from southern Europe. *Proc. Nat. Ac. Sci.* **2007**, *104*, 450–455. [CrossRef] [PubMed]
81. Colombo, F.; Busquets, P.; Ramos, E.; Vergé, S.J.; Ragona, D. Quaternary alluvial terraces in an active tectonic region: The San Juan river valley, Andean ranges, San Juan Province, Argentina. *J. South Am. Earth Sci.* **2000**, *13*, 611–626. [CrossRef]
82. Railsback, L.B.; Gibbard, P.L.; Head, M.J.; Voarintsoa, N.R.G.; Toucanne, S. An optimized scheme of lettered marine isotope substages for the last 1.0 million years, and the climatostratigraphic nature of isotope stages and substages. *Quat. Sci. Rev.* **2015**, *111*, 94–106. [CrossRef]
83. Emery, D.; Myers, K.J. *Sequence Stratigraphy*; Blackwell Science: London, UK, 1996; p. 297.
84. Woolfe, K.J.; Larcombe, P.; Naish, T.; Purdon, R.G. Lowstand rivers need not incise the shelf; an example from the great barrier reef, australia, with implications for sequence stratigraphic models. *Geology* **1988**, *26*, 75–78. [CrossRef]